Phosphorylation-induced SUMOylation promotes Ulk4 condensation at ciliary tip to transduce Hedgehog signal

Mengmeng Zhou[1], Yuhong Han[1], and Jin Jiang[1,2,*]

[1]Department of Molecular Biology, [2]Department of Pharmacology, University of Texas Southwestern Medical Center, Dallas, TX 75390, USA

*Corresponding authors: jin.jiang@utsouthwestern.edu

Abstract

Hedgehog (Hh) signaling controls embryonic development and adult tissue homeostasis through the Gli family of transcription factors. In vertebrates, Hh signal transduction depends on the primary cilium where Gli is thought to be activated at the ciliary tip, but the underlying mechanism has remained poorly understood. Our previous study showed that two Unc-51-like kinase (Ulk) family members Ulk4 and Stk36 colocalize with Gli2 at ciliary tip to promote Gli2 phosphorylation upon Shh stimulation, and that ciliary tip localization of Ulk4/Stk36 depends on phosphorylation of Ulk4 by Stk36 (Zhou et al. 2023). Here we show that phosphorylation of Ulk4 drives its phase separation to form biomolecular condensates that recruit Stk36 and Gli2. Mechanistically, Stk36-mediated phosphorylation of Ulk4 promotes its SUMOylation in response to Shh, and subsequent interaction between SUMO and a SUMO-Interacting-Motif (SIM) in the C-terminal region of Ulk4 drives Ulk4 self-assembly to form biomolecular condensates. Phospho-mimetic mutation of Ulk4 sufficed to drive Ulk4/Stk36/Gli2 condensation at ciliary tip, resulting in constitutive Shh pathway activation. Taken together, our results suggest that phosphorylation-dependent SUMOylation of Ulk4 promotes kinase-substrate condensation at ciliary tip to transduce the Hh signal. We speculate that phase separation driven by phosphorylation-dependent SUMOylation may represent a general mechanism for kinase-mediated signaling.

Introduction

The Hh family glycoproteins play essential roles in embryonic development and adult tissue homeostasis (Jiang and Hui 2008; Briscoe and Therond 2013). Aberrant Hh signaling contributes to a wide range of human diseases including birth defects and cancer (Villavicencio et al. 2000; Nieuwenhuis and Hui 2005; Jiang 2022). Hh signaling in vertebrates critically depends on primary cilia (Goetz and Anderson 2010). In response to Hh stimulation, Hh pathway components including the GPCR family protein and Hh signal transducer Smoothened (Smo) and pathway transcriptional factors Gli proteins accumulate in primary cilia (Corbit et al. 2005; Haycraft et al. 2005; Rohatgi et al. 2007; Chen et al. 2009; Tukachinsky et al. 2010; Chen et al. 2011). Gli proteins are thought to be activated in primary cilia because Gli2 variants that fail to accumulate in the cilia cannot be activated both in cultured cells and in mouse embryos (Santos and Reiter 2014; Liu et al. 2015; Han et al. 2017); however, the underlying mechanism has remained poorly understood.

Our previous studies showed that two Ulk family kinases, Ulk3 and Stk36, act in parallel to convert full-length Gli2 ($Gli2^F$) into its activator form ($Gli2^A$) by directly phosphorylating Gli2 at multiple sites in mammalian cells (Han et al. 2019; Zhou et al. 2022; Zhou and Jiang 2022). More recently, we found that another Ulk family member Ulk4, a pseudokinase, acts in conjunction with Stk36 to promote Gli2 phosphorylation and Hh pathway activation by forming a complex with Stk36 and regulating Stk36 ciliary accumulation (Zhou et al. 2023). Interestingly, we found that Stk36 and Ulk4 depend on

each other for their ciliary localization and that ciliary tip localization of Ulk4 depends on Stk36-mediated phosphorylation of Ulk4 on T1021/T1023 (Zhou et al. 2023).

Here we provide evidence that phosphorylation of Ulk4 by Stk36 drives its phase separation to form biomolecular condensates that recruit Stk36, Gli2 and Sufu. We find that Stk36-mediated phosphorylation of Ulk4 at T1021/T1023 promotes its SUMOylation on an adjacent site (K1030) in response to Shh, and that interaction between SUMO and a SUMO-Interacting-Motif (SIM) in the C-terminal region of Ulk4 drives Ulk4 self-association to form biomolecular condensates. Remarkably, a phospho-mimetic Ulk4 variant can form condensates that recruit Stk36, Gli2 and Sufu in the absence of Shh, leading to constitutive Gli2 phosphorylation and pathway activation.

Results

Phosphorylation of Ulk4 is sufficient to drive its ciliary tip accumulation

Our previous study revealed that phosphorylation of Ulk4 by Stk36 is necessary for its ciliary tip accumulation (Zhou et al. 2023). To determine whether Ulk4 phosphorylation is sufficient to drive its ciliary tip accumulation, we generated a phospho-mimetic form of human Ulk4 (hUlk4) by converting two previously identified Stk36 sites (T1021 and T1023) to E (Ulk4-EE). C-terminally HA-tagged wild type Ulk4 (Ulk4-WT) and Ulk4-EE were expressed in NIH3T3 cells via lentiviral infection, followed by Shh stimulation. As shown in Figure 1A, Ulk4-WT-HA accumulated at ciliary tip only after Shh stimulation whereas Ulk4-EE-HA accumulated at ciliary tip regardless of Shh treatment. Quantification of ciliary tip Ulk4 signals revealed that Shh dramatically increased Ulk4-

95 WT-HA levels but had little if any effect on Ulk4-EE-HA levels at ciliary tips (Figure 1B),
96 suggesting that Stk36-mediated phosphorylation of Ulk4 is sufficient to promote its
97 ciliary tip accumulation.

98 We next asked whether Ulk4-EE could bring Stk36 to the ciliary tip in the
99 absence of Shh. NIH3T3 cells were infected with lentivirus expressing Myc-tagged
100 Stk36 (Myc-Stk36) and Ulk4-WT-HA or Ulk4-EE-HA, followed by immunostaining with
101 antibodies against the epitope tags to monitor ciliary accumulation of Myc-Stk36 and
102 Ulk4-WT-HA/Ulk4-EE-HA. Cells co-expressing Myc-Stk36 and Ulk4-WT-HA showed no
103 ciliary tip accumulation of either Ulk4-WT-HA or Myc-Stk36 (Figure1C and D). By
104 contrast, cells co-expressing Myc-Stk36 and Ulk4-EE-HA showed ciliary tip
105 accumulation of both Ulk4-EE-HA and Myc-Stk36 (Figure1C and D), suggesting that
106 Ulk4-EE could bring Stk36 to the ciliary tip even in the absence of Shh.

107
108
109 **Gli2 ciliary tip accumulation is promoted by Stk36/Ulk4**
110
111 In response to Shh, Gli proteins and their binding partner and Hh pathway inhibitor Sufu
112 accumulate at ciliary tip while Smo accumulates along the cilium axoneme (Corbit et al.
113 2005; Haycraft et al. 2005; Rohatgi et al. 2007; Chen et al. 2009; Tukachinsky et al.
114 2010; Chen et al. 2011). The mechanisms that control ciliary tip localization of Gli
115 proteins are poorly understood although Kif7/Gli interaction has been implicated to play
116 an important role (Haque et al. 2022). The observations that Stk36/Ulk4 colocalized with
117 Gli2 at ciliary tip and that Ulk family kinases including Ulk3 and Stk36 acted upstream of
118 Gli2 to promote Shh pathway activation let us to speculate that Gli ciliary tip localization
119 could be regulated by these kinases. Indeed, as shown in Figure 2A and B, Shh-

120 induced ciliary accumulation of Gli2 and Sufu was diminished in Stk36 and Ulk3 double
121 knockout (DKO) NIH3T3 cells (NIH3T3^{DKO}) (Han et al. 2019). Expression of wild type
122 Stk36 (Stk36-WT) but not its kinase inactive form (Stk36-AA; Zhou et al. 2023) restored
123 ciliary tip accumulation of both Gli2 and Sufu in response to Shh (Figure 2A and B).
124 Furthermore, expression of Ulk4-EE but not Ulk4-WT in NIH3T3^{DKO} cells restored ciliary
125 tip localization of both Gli2 and Sufu, which correlated with ciliary localization of Ulk4-EE
126 (Figure 2C-F). These results suggest ciliary tip localization of Glli2 and Sufu is promoted
127 by Stk36 and Ulk4.
128
129
130 **Phosphorylation drives Ulk4 condensation**
131
132 The ciliary tip accumulation of Hh signaling components resembles biomolecular
133 condensate formation that depends on multivalent interactions and protein
134 concentrations (Banani et al. 2017; Shin and Brangwynne 2017). Indeed, Stk36, Ulk4,
135 Gli and Sufu physically interact with one another (Han et al. 2015; Preuss et al. 2020;
136 Zhou et al. 2023). Upon Hh stimulation, Smo is accumulated and activated in primary
137 cilia, which may result in local activation of Stk36 kinase and Stk36-mediated
138 phosphorylation of Ulk4, leading to their condensation that also recruits Gli2/Sufu. To
139 test this hypothesis, we asked whether Stk36-mediated phosphorylation of Ulk4 can
140 drive Stk36/Ulk4 condensation in the cytoplasm when both proteins were
141 overexpressed in HEK293T cells. Constitutively active Stk36 (Stk36-EE) or its kinase
142 inactive form (Stk36-AA) was transfected into HEK293T cells together with Ulk4-WT. As
143 shown in Figure 3A, coexpression of Stk36-EE with Ulk4-WT led to the formation of
144 Ulk4 puncta that also contained Stk36. However, coexpression of Stk36-AA with Ulk4-

145 WT failed to induce the formation of Ulk4/Stk36 puncta. The formation of Ulk4/Stk36
146 puncta depends on phosphorylation of Ulk4 by Stk36 because HEK293T cells co-
147 expressing a phospho-deficient form of Ulk4 (Ulk4-2TA) and Stk36-EE failed to form
148 Ulk4/Stk36 puncta (Figure 3B). Strikingly, HEK293T cells expressing Ulk4-EE formed
149 Ulk4 condensates that also recruited endogenous Gli2 and Sufu into the condensates
150 (Figure 3C). These results suggest that phosphorylation of Ulk4 by Stk36 promotes the
151 formation of Ulk4 condensates that can recruit its interaction proteins including Stk36,
152 Gli2 and Sufu.
153 Most membraneless biomolecular condensates form through Liquid-Liquid phase
154 separation (LLPS) that can be disrupted by 1, 6-hexanediol (Sabari et al. 2018;
155 McKnight 2024). Indeed, the condensates of GFP-tagged YAP (GFP-YAP), which is
156 formed via LLPS (Cai et al. 2019), were disrupted by treating cells with 5% 1, 6-
157 hexanediol for 5 min (Figure 3D). To determine the biomaterial property of the
158 condensates organized by Ulk4, we treated HEK293T cells that contained CFP-
159 Stk36/Ulk4-EE condensates with 5% 1, 6-hexanediol for 5 to 30 minutes. We found that
160 CFP-Stk36/Ulk4-EE condensates were resistant to 1, 6-hexanediol even after treatment
161 for 30 min (Figure 3D; Figure 3- figure supplement 1), suggesting that Stk36/Ulk4
162 condensates are more rigid than LLPS and may resemble gel-like or solid-state
163 condensates (Woodruff et al. 2017; Putnam et al. 2019).
164
165
166 **Shh induces SUMOylation of Ulk4 depending on Stk36-mediated phosphorylation**
167
168 We next asked how Ulk4 phosphorylation promotes its condensation. Phosphorylation
169 can regulate other post-translational modifications (PTMs) such as SUMOylation, and

170 SUMOylation has been implicated in the formation of biomolecular condensates (Shen
171 et al. 2006; Yang and Gregoire 2006; Keiten-Schmitz et al. 2021). Interestingly, like
172 Ulk4-mediated condensation, condensates formed by a synthetic construct containing
173 multiple SUMO and SIM domains, RFP-SUMO6-SIM10 (Banani et al. 2016), were also
174 resistant to 1, 6-hexanediol treatment (Figure 3D; Figure 3- figure supplement 1).
175 Therefore, we asked whether phosphorylation induces Ulk4 condensation through
176 promoting its SUMOylation. Coexpression of Ulk4-HA with Fg-Stk36-EE but not with Fg-
177 Stk36-AA in HEK293T cells resulted in a mobility shift of Ulk4-HA indicative of SUMO
178 conjugation (Figure 4A; top panel). Probing with anti-SUMO1 antibody confirmed that
179 higher molecular weight bands contained SUMOylated Ulk4 (Figure 4A; bottom panel).
180 Mutating the Stk36 sites on Ulk4 (Ulk4-2TA) abolished Ulk4 SUMOylation stimulated by
181 Stk36-EE (Figure 4B). On the other hand, Ulk4-EE was SUMOylated without
182 coexpression of Stk36-EE, and SUMOylation of Ulk4-EE was abolished by a
183 SUMOylation inhibitor TAK981 (Fig. 4C)(Langston et al. 2021). These results
184 demonstrated that Stk36-mediated phosphorylation at T1021/T1023 can induce Ulk4
185 SUMOylation. Of note, SUMOylated Ulk4 tends to form high molecular weight species
186 on the SDS-PAGE, a phenomenon also observed for SUMOylated nuclear hormone
187 receptors (Poukka et al. 2000; Tian et al. 2002).
188 To determine whether Shh induces SUMOylation of Ulk4 depending on its
189 phosphorylation by Stk36, Ulk4-WT or Ulk4-2TA was expressed in NIH3T3 cells via
190 lentiviral infection, followed by Shh stimulation. As shown in Figure 4D, Shh induced
191 SUMOylation of Ulk4-WT but not Ulk4-2TA.

192 SUMOylation sites have consensus motifs: ψKxE/D or E/DxKψ, where ψ is a
193 large hydrophobic amino acid and x could be any amino acid (Matic et al. 2010).
194 SUMOylation of many proteins was promoted by phosphorylation on sites adjacent to
195 the SUMOylation sites (Yang and Gregoire 2006). Inspection of Ulk4 C-terminal region
196 identified a SUMOylation consensus site ($ESK_{1030}L$) adjacent to the Stk36
197 phosphorylation sites (Figure 4E). To determine whether phosphorylation of Ulk4 at
198 T1021/T1023 could promote SUMOylation at K1030, we carried out *in vitro*
199 SUMOylation experiments. GST fusion proteins containing a Ulk4 fragment that
200 encompasses both the Stk36 sites and the putative SUMOylation site (GST-Ulk4C;
201 Figure 4E) were incubated with immunopurified Stk36-EE and recombinant CK1 for *in*
202 *vitro* phosphorylation, followed by incubation with SUMO1 and SUMO enzymes (E1 and
203 E2) for *in vitro* SUMOylation. As shown in Figure 4F, GST-Ulk4C was SUMOylated after
204 kinase phosphorylation. Of note, CK1 was included to boost Stk36 kinase activity in the
205 *in vitro* phosphorylation assay. Mutation of either K1030 to R (KR) or T1021/T1023 to
206 A/A (2TA) abolished *in vitro* SUMOylation of GST-Ulk4C (Figure 4F). Furthermore, the
207 K1030R mutation abolished Stk36-induced SUMOylation of Ulk4 and the constitutive
208 SUMOylation of Ulk4-EE (Ulk4-EE-KR) in HEK293T cells, as well as Shh-induced Ulk4
209 SUMOylation in NIH3T3 cells (Figure 4G-I). Taken together, these results demonstrate
210 that Shh induces SUMOylation of Ulk4 on K1030 depending on its phosphorylation at
211 T1021/T1023.
212
213 **SUMOylation promotes Ulk4 self-association via SUMO/SIM interaction**

214 SUMOylation mediates protein-protein interaction by binding to SIM, which consists of a
215 stretch of hydrophobic amino acids adjacent to acidic residues (Song et al. 2004).
216 Interestingly, Ulk4 contains a SIM motif ($_{1145}$EDLLLL$_{1151}$DLE) located C-terminally to
217 phosphorylation-mediated SUMOylation site (Figure. 4E). To determine whether
218 SUMOylation of Ulk4 promotes its self-association through interacting with SIM, we
219 examined the interaction between Flag-tagged Ulk4-EE (Ulk4-EE-Fg), which is
220 constitutively SUMOylated, or Ulk4-EE-KR-Fg, which is no longer SUMOylated (Figure
221 4H), with HA-tagged wild type (Ulk4-WT-HA) or SIM-deficient Ulk4 (Ulk4-ΔSIM-HA;
222 Figure. 4E). These constructs were transfected into HEK293T cells, followed by co-
223 immunoprecipitation (Co-IP) and western blot analysis. As shown in Figure 4J, Ulk4-EE-
224 Fg formed a complex with Ulk4-WT-HA, which was diminished when SIM was mutated
225 in Ulk4-WT-HA (Ulk4-ΔSIM-HA) or the SUMOylation site was mutated in Ulk4-EE-Fg
226 (Ulk4-EE-KR-Fg). We also generated a C-terminal fragment of Ulk4-EE from aa1004-
227 aa1275 of (C272-EE-Fg). C272-EE-Fg formed a complex with Ulk4-WT-HA albeit at
228 lower affinity compared with Ulk4-EE-Fg; however, C272-EE-Fg failed to form a
229 complex with Ulk4-ΔSIM-HA (Figure 4K). These observations suggest that 1) SUMO-
230 SIM interaction facilitates Ulk4 self-association through its C-terminal region and 2) the
231 N-terminal region of Ulk4 can also mediate Ulk4 self-association independent of SUMO-
232 SIM interaction.
233
234 **SUMOylation and SIM are essential for Ulk4 condensation and Ulk4-mediated Shh**
235 **pathway activation**

236 To determine whether SUMOylation and SIM mediates Ulk4 condensation as is the
237 case for PLM bodies (Shen et al. 2006), we coexpressed Stk36-EE with wild type (Ulk4-
238 WT), SUMOylation deficient (Ulk4-KR), or SIM mutated Ulk4 (Ulk4-ΔSIM) in HEK293T
239 cells. As shown in Figure 5A, while Ulk4-WT formed condensates that contained Stk36-
240 EE, neither Ulk4-KR nor Ulk4-ΔSIM formed condensates but rather exhibited diffused
241 distribution in HEK293T cells.

242 Next, we expressed human Ulk4-WT, Ulk4-KR, or Ulk4-ΔSIM via lentiviral
243 infection in NIH3T3 cells with endogenous Ulk4 depleted by shRNA and treated the
244 cells with or without Shh. In contrast to Ulk4-WT, which was accumulated at the ciliary
245 tip after Shh treatment, neither Ulk4-KR nor Ulk4-ΔSIM accumulated at ciliary tip in
246 response to Shh stimulation (Figure 5B and C). While Ulk4-WT rescued Gli2
247 phosphorylation, *Ptch1* and *Gli1* expression induced by Shh in Ulk4 depleted cells,
248 neither Ulk4-KR nor Ulk4-ΔSIM rescued Gli2 phosphorylation and Shh target gene
249 expression (Figure 5D-F). These results suggest that Shh-induced Ulk4 SUMOylation
250 and subsequent SUMO-SIM interaction is essential for Ulk4 condensation at ciliary tip
251 and its role in mediating Shh pathway activation.

252

253 **Ulk4-EE exhibits constitutive pathway activity depending on its SUMOylation**

254 Ulk4-EE formed condensates in the cytoplasm when expressed in HEK293T cells and
255 accumulated at the ciliary tips in NIH3T3 cells in the absence of Shh. Treating cells with
256 the SUMOylation inhibitor TAK-981 abolished Ulk4 condensation and ciliary tip
257 accumulation (Figure 6A-C), suggesting that Ulk4-EE condensation and constitutive
258 ciliary tip localization may depend on its SUMOylation. To determine whether Ulk4-EE

259 condensation and constitutive ciliary tip localization depend on its SUMOylation at
260 K1030, we examined Ulk4-EE-KR-Fg in which K1030 was mutated to R. In contrast to
261 Ulk4-EE-Fg, Ulk4-EE-KR-Fg neither formed condensates in HEK293T cells nor
262 accumulated at ciliary tip when expressed in NIH3T3 cells (Figure 6D-F).

263 Consistent with its constitutive ciliary tip accumulation and its ability to recruit
264 Stk36 and Gli2/Sufu to the ciliary tip (Figure 1A, C and Figure 2C-F), Ulk4-EE also
265 exhibited constitutive pathway activity as indicated by Gli2 phosphorylation and
266 transcriptional activation of *Ptch1* and *Gli1* in the absence of Shh (Figure 6G-L).
267 Blocking the SUMOylation of Ulk4-EE with either TAK-981 treatment or the K1030R
268 mutation inhibited its constitutive pathway activity (Figure 6G-L). Knockdown of Stk36
269 attenuated Shh-independent activation of *Ptch1* and *Gli1* induced by Ulk4-EE (Figure 7-
270 figure supplement 1A and B), suggesting that the constitutive pathway activity of Ulk4-
271 EE depends on Stk36. Indeed, Ulk4-EE could activate Stk36 as indicated by the
272 phosphorylation of the activation loop in the Stk36 kinase domain (p158T/pS1590;
273 Figure 7-figure supplement 1C) even though Stk36 is normally activated by Shh
274 independent of Ulk4 (Zhou et al. 2023). Taken together, these results suggest that
275 phosphorylation-mediated SUMOylation and subsequent SUMO-SIM interaction drives
276 Ulk4 condensation that recruits Stk36 and Gli2 at ciliary tip, which is essential for Ulk4's
277 role in mediating Shh signal transduction.

278
279
280 **Discussion**
281
282
283 How Hh converts the latent Gli transcription factor into its activator form at ciliary tip has
284 remained an enigma in the field. Our previous study revealed that Stk36/Ulk4 acts in

285 parallel with Ulk3 to promote Gli2 phosphorylation and activation in a manner depending
286 on ciliary tip localization of Stk36/Ulk4, and that Shh-induced ciliary tip accumulation of
287 this kinase/pseudokinase pair depends on phosphorylation of Ulk4 by Stk36 (Zhou et al.
288 2023). Here we demonstrate that phosphorylation of Ulk4 induces its SUMOylation and
289 that subsequent SUMO-SIM mediated protein-protein interaction promotes ciliary tip
290 condensation of Ulk4 that also recruits Stk36 and Gli2-Sufu, leading to Gli2
291 phosphorylation and activation (Figure 7). We further showed that Shh-induced
292 SUMOylation of Ulk4 depended on Ulk4 phosphorylation at T1021/T1023 and that a
293 phospho-mimetic Ulk4 variant (Ulk4-EE) formed condensates that recruited Stk36 and
294 Gli2 in the absence of Shh, leading to constitutive pathway activation.

295 Biomolecular condensates have been implicated in many cellular processes in
296 which they function to facilitate biochemical reactions by simultaneously concentrating
297 substrates and enzymes in the same subcellular compartments (Banani et al. 2017;
298 Shin and Brangwynne 2017; Su et al. 2021). The formation of biomolecular
299 condensates through phase separation is often constitutive or regulated in response to
300 stress signals. Whether phase separation can be induced by extracellular signals such
301 as morphogens has been largely underexplored. Here we showed that Shh induces the
302 formation of Ulk4 condensates that recruit Stk36 and Gli2 at ciliary tip to facilitate Gli2
303 phosphorylation and activation, providing a mechanistic insight into how Shh activates
304 Gli proteins at ciliary tip. The formation of Stk36-Ulk4-Gli2 condensates at ciliary tip in
305 response to Shh stimulation is likely due to local activation of Stk36 kinase by activated
306 Smo accumulated at primary cilia and relatively high concentration of Stk36, Ulk4, Gli2
307 and Sufu at ciliary tips. Indeed, overexpression of Ulk4-EE or Stk36-EE/Ulk4 in

308 HEK293T cells led to the formation of Stk36/Ulk4 condensates in the cytoplasm that
309 could also recruit endogenous Gli2 and Sufu.

310 In most cases, the formation of membraneless biomolecular condensates is
311 driven by liquid-liquid phase separation (LLPS) mediated through intrinsically disordered
312 regions (IDRs)/low-complexity domains (LCDs) (Banani et al. 2017; Shin and
313 Brangwynne 2017). Here we showed that phosphorylation-regulated SUMOylation of
314 Ulk4 and subsequent SUMO-SIM interaction is responsible for Shh-induced
315 Stk36/Ulk4/Gli2 condensation at ciliary tip, which provides a mechanism that links
316 kinase-mediated signaling and biomolecular condensation. Because phosphorylation-
317 induced SUMOylation motifs are present in many regulatory proteins (Yang and
318 Gregoire 2006), and SUMOylation has been implicated as a mechanism for condensate
319 formation (Keiten-Schmitz et al. 2021), we speculate that phase separation driven by
320 phosphorylation-dependent SUMOylation could be generally utilized in other settings
321 and may represent a more general mechanism for kinase-mediated signaling.

322 Unlike liquid-like condensates whose formation is mediated by IDRs/LCDs and
323 can be disrupted by 1,6 Hexanediol (Sabari et al. 2018; McKnight 2024),
324 Ulk4/Stk36/Gli2 condensates are resistant to 1,6 Hexanediol treatment (Figure 3D;
325 Figure 3-figure supplement 1), thus may resemble gel-like or solid-state condensates
326 (Woodruff et al. 2017; Putnam et al. 2019). Interestingly, SUMO/SIM-mediated
327 condensation of a synthetic construct (RFP-SUMO6-SIM10) also formed gel-like/solid-
328 state condensates because they were resistant to 1,6 Hexanediol treatment (Figure 3D;
329 Figure 3-figure supplement 1). It would be interesting to determine whether other

330 condensates mediated by SUMO-SIM interaction such as PLM also exhibit gel-
331 like/solid-state property.
332 Although Shh-induced SUMOylation of Ulk4 and SUMO-SIM-mediated
333 interaction are essential for the formation of Ulk4/Stk36/Gli2/Sufu condensates, other
334 protein-protein interaction events could also be important for the ciliary tip accumulation
335 of these intracellular Hh signaling components. Indeed, a recent study revealed that
336 Kif7-Gli2 interaction is essential for their ciliary tip accumulation (Haque et al. 2022). In
337 the future, it would be interesting to explore the functional relationship between Kif7 and
338 the Ulk family kinases in the regulation of ciliary accumulation of Gli proteins.
339
340
341
342

343 **Materials and methods**

344

345 **DNA constructs**

346 Myc-Gli2 was described previously (Han et al. 2019). Myc-Stk36, Fg-Stk36-WT, Fg-
347 Stk36-EE, Fg-Stk36-AA, Ulk4-WT-HA, Ulk4-AA-HA, GST-Ulk4C-WT, GST-Ulk4C-2TA
348 were generated previously (Zhou et al. 2023). C-terminally 3XHA-tagged human Ulk4-
349 EE, Ulk4-KR, Ulk4-ΔSIM and C-terminally 3XFg-tagged Ulk4-EE, Ulk4-EE-KR, Ulk4-
350 C272-EE were subcloned into the *FUGW* vector between EcoRI and BamHI sites. All
351 GST fusion proteins were subcloned into the *pGEX 4T-1* vector between EcoRI and
352 XhoI sites. Ulk4C-KR, Ulk4-C272-EE, Ulk4-KR, Ulk4-ΔSIM, Ulk4-EE, Ulk4-EE-KR
353 plasmids were constructed by PCR-mediated site-directed mutagenesis.

354

355 **Cell culture, transfection, and Shh treatment**

356 NIH3T3 cells (ATCC, CRL-1658) were cultured in Dulbecco's modified Eagle's medium
357 (DMEM, Sigma) with10% bovine calf serum (BCS, Gibco) and 1% penicillin-
358 streptomycin (Sigma). GenJet Plus *in vitro* DNA transfection kit was used for
359 transfection experiments according to the manufacturer's instruction (SignaGen).
360 HEK293T cells (ATCC, CRL-11268) were cultured in DMEM containing 10% fetal bovine
361 serum (FBS, Gibco) and 1% penicillin-streptomycin. Transfection was performed using
362 the PolyJet *in vitro* DNA transfection kit (SignaGen) according to the instruction. For Shh
363 treatment, the NIH3T3 cells were cultured at 50%-confluent densities in plate or
364 chamber slides for one day and starved in serum-free medium (0.5% BCS) for 12 hours
365 to allow ciliation. The recombinant human Shh N-terminal fragment (1 ng/ml; R&D

366 Systems, #8908-SH-005) was then added to the same serum-free medium for 12 hours
367 or overnight.
368
369 **Immunostaining, immunoprecipitation, and western blotting analysis**
370 Immunostaining and quantification were carried out as previously described (Han et al.
371 2019; Zhou et al. 2023). Images were captured using Zeiss LSM700 laser scanning
372 microscope. Fluorescence signal intensities were measured in the respective channel
373 by ImageJ. 20 cells were randomly picked for each experimental group to measure
374 ciliary tip fluorescence signal intensities. For Co-IP experiments were carried out as
375 previously described (Zhou et al. 2023). Western blot was carried out using standard
376 protocol as previously described (Zhou et al. 2023). Antibodies used in this study were
377 as follows: Mouse anti-Myc (Santa Cruz Biotechnology; 9E10), Mouse anti-Flag (Sigma;
378 M2), Mouse anti-HA (Santa Cruz Biotechnology; F7), Mouse anti-acetylated Tubulin
379 (Sigma; T7451; staining:1:1000), Rabbit anti-Myc (Abcam; ab9106; staining 1:2000),
380 Rabbit anti-HA (AbCam; ab9110; staining 1:500), Rabbit anti-SUMO1 (4930, Cell
381 Signaling), Rabbit anti-Sufu (Abcam;ab28083; staining 1:500). Goat anti-HA (NOVUS;
382 NB600-362; 1:400), Goat anti-Gli2 (R&D system; AF3635; staining 1:1000), Rabbit anti-
383 pGli2 (pS230/232) (Han et al. 2019), and Rabbit anti-pStk36 (pT158/pS159) (Shi et al.
384 2011; Zhou et al. 2023)
385
386 **SUMOylation Assay**
387 Cell-based SUMOylation assay was carried out as previously described (Ma et al. 2016;
388 Han and Jiang 2022). Briefly, cell pellets were lysed at 4 °C for 10 min with lysis buffer

389 containing 20 mM Tris HCl pH 8.0, 150 mM NaCl, 5 mM EDTA, 1% IGPAL CA-630, 10%
390 glycerol, 1 mM DTT, 20 mM NEM, 1X protease inhibitors cocktail, 1X phosSTOP
391 phosphatase inhibitors. SDS was added into the lysates to a final concentration of 1%
392 and the mixture was boiled 5 min. After 5-fold dilution with cool lysis buffer, the mixture
393 was subjected to immunoprecipitation and western blot analysis.

394 *In vitro* SUMOylation experiments were performed using the SUMOylation Assay
395 Kit (Abcam; ab139470) following manufacturer's instruction. Flag-tagged Stk36-EE was
396 transiently expressed in HEK293T cells, purified with anti-Fg agarose (Sigma; A2220)
397 and eluted with Flag peptide (Sigma; F4799). The GST and GST fusion proteins were
398 purified with glutathione beads (GE; 17-0756-01) and the resulting agarose were
399 subjective to phosphorylation by Stk36-EE/CK1 as previously described (Zhou et al.
400 2022). The products of *in vitro* kinase assays were used as the substrates for *in vitro*
401 SUMOylation assays.

402

403 **1,6 hexanediol treatment**

404 Cultured HEK293T cells were transfected with GFP-Stk36 and Ulk4-EE-HA, GFP-YAP
405 or RFP-SUMO6SIM10 DNA constructs. After 48 hours, cells were treated with 5% 1,6
406 hexanediol for 5-30 minutes. Images were taken before and after treatment.

407

408 **Lentivirus production and infection**

409 To package the lentivirus, Ulk4 shRNA vector or *FUGW* lentiviral constructs were co-
410 transfected with packaging plasmids (PSPAX2 and PMDG2) into HEK293T cells using

411 PolyJet. After 48 hours to 72 hours of incubation, the supernatant was transferred to a
412 15 mL centrifuge tube and centrifuged at 2500 RPM for 15 minutes. After filtered
413 through a 0.45 mM filter, the supernatant was collected into a new sterile tube
414 (Beckman; 344059) and centrifuged at 20,000 g for 2 hours. The sediment was re-
415 suspended, aliquoted in small volume of 10% FBS culture medium and stored at -80°C
416 for future use. For cell infection, lentiviruses were added to 70% confluent wild type
417 NIH3T3 cells together with Polybrene (Sigma, Cat. No. H9268) for overnight to get
418 stable NIH3T3 cell lines.

419

420 **RNA interference**

421 The mouse Ulk4 shRNA lentiviral vector was purchased from Sigma (Sigma;
422 TRCN0000328268). The Non target shRNA Plasmid DNA (Sigma; SHC016) was used
423 as a control. The target sequence of mouse Ulk4 shRNA is:
424 CTGCGAAGATTATCGAGAATG. The sequences for Stk36 siRNA were: 5'-
425 GGUAUACUGGCUUCAGAAA-3' (Cat# SASI_ Mm02 _00345637) and 5'-
426 GCCUUAUGUGCUUUGCUGU-3' (Cat# SASI_Mm01_00167751). The sequences for
427 negative control were: 5'-UUCUCCGAACGUGUCACG U-3'. The knockdown efficiency
428 was validated via real-time PCR.

429

430 **Quantitative RT-qPCR**

431 Total RNA was extracted from 1 × 10^6 cells using the RNeasy Plus Mini Kit (Qiagen;
432 74134), and cDNA was synthesized with High-Capacity cDNA Reverse Transcription Kit

433 (Applied Biosystems; 01279158) and qPCR was performed using Fast SYBR Green
434 Master Mix (Applied Biosystems; 2608088) and a Bio-Rad CFX96 real-time PCR
435 system (BIO-RAD; HSP9601). The RT-qPCR was performed in triplicate for each of
436 three independent biological replicates. Quantification of mRNA levels was calculated
437 using the comparative CT method. Primers: Gli1, 5'-GTGCACGTTTGAAGGCTGTC-3'
438 and 5'-GAGTGGGTCCGATTCTGGTG-3'; Ptch1, 5'-GAAGCCACAGAAAACCCTGTC-3'
439 and 5'-GCCGCAAGCCTTCTCTACG-3'; Ulk4, 5'- ATGCAGAGTGTGATTGCGTTG-3'
440 and 5'- GAGTGGCAGTTTCTGTGAACA-3'; Stk36, 5'-
441 CGCATCCTACACCGAGATATGA-3' and 5'- AAATCCAAAGTCACAGAGCTTGA-3';
442 GAPDH, 5'-GTGGTGAAGCAGGCATCTGA-3' and 5'-GCCATGTAGGCCATGAGGTC-
443 3'.
444

445 **Acknowledgements**
446 We thank Bing Wang and Yong Suk Cho for helps during performing the experiments.
447 J. Jiang is a Eugene McDermott Endowed Scholar in Biomedical Science at the
448 University of Texas Southwestern.
449
450
451 **Declaration of interests**
452
453 The authors declare no competing interests.
454
455

456 **Reference**

457

458 Banani SF, Lee HO, Hyman AA, Rosen MK. 2017. Biomolecular condensates:
459 organizers of cellular biochemistry. *Nat Rev Mol Cell Biol* **18**: 285-298.
460 Banani SF, Rice AM, Peeples WB, Lin Y, Jain S, Parker R, Rosen MK. 2016.
461 Compositional Control of Phase-Separated Cellular Bodies. *Cell* **166**: 651-663.
462 Briscoe J, Therond PP. 2013. The mechanisms of Hedgehog signalling and its roles in
463 development and disease. *Nat Rev Mol Cell Biol* **14**: 418-431.
464 Cai D, Feliciano D, Dong P, Flores E, Gruebele M, Porat-Shliom N, Sukenik S, Liu Z,
465 Lippincott-Schwartz J. 2019. Phase separation of YAP reorganizes genome
466 topology for long-term YAP target gene expression. *Nat Cell Biol* **21**: 1578-1589.
467 Chen MH, Wilson CW, Li YJ, Law KK, Lu CS, Gacayan R, Zhang X, Hui CC, Chuang
468 PT. 2009. Cilium-independent regulation of Gli protein function by Sufu in
469 Hedgehog signaling is evolutionarily conserved. *Genes Dev* **23**: 1910-1928.
470 Chen Y, Sasai N, Ma G, Yue T, Jia J, Briscoe J, Jiang J. 2011. Sonic Hedgehog
471 dependent phosphorylation by CK1alpha and GRK2 is required for ciliary
472 accumulation and activation of smoothened. *PLoS biology* **9**: e1001083.
473 Corbit KC, Aanstad P, Singla V, Norman AR, Stainier DY, Reiter JF. 2005. Vertebrate
474 Smoothened functions at the primary cilium. *Nature* **437**: 1018-1021.
475 Goetz SC, Anderson KV. 2010. The primary cilium: a signalling centre during vertebrate
476 development. *Nat Rev Genet* **11**: 331-344.
477 Han Y, Jiang J. 2022. Cell-Based Assays for Smoothened Ubiquitination and
478 Sumoylation. *Methods Mol Biol* **2374**: 139-147.

479 Han Y, Shi Q, Jiang J. 2015. Multisite interaction with Sufu regulates Ci/Gli activity
480 through distinct mechanisms in Hh signal transduction. *Proc Natl Acad Sci U S A*
481 **112**: 6383-6388.
482 Han Y, Wang B, Cho YS, Zhu J, Wu J, Chen Y, Jiang J. 2019. Phosphorylation of Ci/Gli
483 by Fused Family Kinases Promotes Hedgehog Signaling. *Dev Cell* **50**: 610-626
484 e614.
485 Han Y, Xiong Y, Shi X, Wu J, Zhao Y, Jiang J. 2017. Regulation of Gli ciliary localization
486 and Hedgehog signaling by the PY-NLS/karyopherin-beta2 nuclear import
487 system. *PLoS biology* **15**: e2002063.
488 Haque F, Freniere C, Ye Q, Mani N, Wilson-Kubalek EM, Ku PI, Milligan RA,
489 Subramanian R. 2022. Cytoskeletal regulation of a transcription factor by DNA
490 mimicry via coiled-coil interactions. *Nat Cell Biol* **24**: 1088-1098.
491 Haycraft CJ, Banizs B, Aydin-Son Y, Zhang Q, Michaud EJ, Yoder BK. 2005. Gli2 and
492 gli3 localize to cilia and require the intraflagellar transport protein polaris for
493 processing and function. *PLoS Genet* **1**: e53.
494 Jiang J. 2022. Hedgehog signaling mechanism and role in cancer. *Semin Cancer Biol*
495 **85**: 107-122.
496 Jiang J, Hui CC. 2008. Hedgehog signaling in development and cancer. *Dev Cell* **15**:
497 801-812.
498 Keiten-Schmitz J, Roder L, Hornstein E, Muller-McNicoll M, Muller S. 2021. SUMO:
499 Glue or Solvent for Phase-Separated Ribonucleoprotein Complexes and
500 Molecular Condensates? *Front Mol Biosci* **8**: 673038.

501 Langston SP, Grossman S, England D, Afroze R, Bence N, Bowman D, Bump N, Chau
502 R, Chuang BC, Claiborne C et al. 2021. Discovery of TAK-981, a First-in-Class
503 Inhibitor of SUMO-Activating Enzyme for the Treatment of Cancer. *J Med Chem*
504 **64**: 2501-2520.
505 Liu J, Zeng H, Liu A. 2015. The loss of Hh responsiveness by a non-ciliary Gli2 variant.
506 *Development* **142**: 1651-1660.
507 Ma G, Li S, Han Y, Li S, Yue T, Wang B, Jiang J. 2016. Regulation of Smoothened
508 Trafficking and Hedgehog Signaling by the SUMO Pathway. *Dev Cell* **39**: 438-
509 451.
510 Matic I, Schimmel J, Hendriks IA, van Santen MA, van de Rijke F, van Dam H, Gnad F,
511 Mann M, Vertegaal AC. 2010. Site-specific identification of SUMO-2 targets in
512 cells reveals an inverted SUMOylation motif and a hydrophobic cluster
513 SUMOylation motif. *Mol Cell* **39**: 641-652.
514 McKnight SL. 2024. Protein domains of low sequence complexity-dark matter of the
515 proteome. *Genes Dev* **38**: 205-212.
516 Nieuwenhuis E, Hui CC. 2005. Hedgehog signaling and congenital malformations. *Clin*
517 *Genet* **67**: 193-208.
518 Poukka H, Karvonen U, Janne OA, Palvimo JJ. 2000. Covalent modification of the
519 androgen receptor by small ubiquitin-like modifier 1 (SUMO-1). *Proc Natl Acad*
520 *Sci U S A* **97**: 14145-14150.
521 Preuss F, Chatterjee D, Mathea S, Shrestha S, St-Germain J, Saha M, Kannan N,
522 Raught B, Rottapel R, Knapp S. 2020. Nucleotide Binding, Evolutionary Insights,

523 and Interaction Partners of the Pseudokinase Unc-51-like Kinase 4. *Structure* **28**:
524 1184-1196 e1186.
525 Putnam A, Cassani M, Smith J, Seydoux G. 2019. A gel phase promotes condensation
526 of liquid P granules in Caenorhabditis elegans embryos. *Nat Struct Mol Biol* **26**:
527 220-226.
528 Rohatgi R, Milenkovic L, Scott MP. 2007. Patched1 regulates hedgehog signaling at the
529 primary cilium. *Science* **317**: 372-376.
530 Sabari BR, Dall'Agnese A, Boija A, Klein IA, Coffey EL, Shrinivas K, Abraham BJ,
531 Hannett NM, Zamudio AV, Manteiga JC et al. 2018. Coactivator condensation at
532 super-enhancers links phase separation and gene control. *Science* **361**.
533 Santos N, Reiter JF. 2014. A central region of Gli2 regulates its localization to the
534 primary cilium and transcriptional activity. *J Cell Sci* **127**: 1500-1510.
535 Shen TH, Lin HK, Scaglioni PP, Yung TM, Pandolfi PP. 2006. The mechanisms of PML-
536 nuclear body formation. *Mol Cell* **24**: 331-339.
537 Shi Q, Li S, Jia J, Jiang J. 2011. The Hedgehog-induced Smoothened conformational
538 switch assembles a signaling complex that activates Fused by promoting its
539 dimerization and phosphorylation. *Development* **138**: 4219-4231.
540 Shin Y, Brangwynne CP. 2017. Liquid phase condensation in cell physiology and
541 disease. *Science* **357**.
542 Song J, Durrin LK, Wilkinson TA, Krontiris TG, Chen Y. 2004. Identification of a SUMO-
543 binding motif that recognizes SUMO-modified proteins. *Proceedings of the*
544 *National Academy of Sciences of the United States of America* **101**: 14373-
545 14378.

546 Su Q, Mehta S, Zhang J. 2021. Liquid-liquid phase separation: Orchestrating cell
547 signaling through time and space. *Mol Cell* **81**: 4137-4146.
548 Tian S, Poukka H, Palvimo JJ, Janne OA. 2002. Small ubiquitin-related modifier-1
549 (SUMO-1) modification of the glucocorticoid receptor. *Biochem J* **367**: 907-911.
550 Tukachinsky H, Lopez LV, Salic A. 2010. A mechanism for vertebrate Hedgehog
551 signaling: recruitment to cilia and dissociation of SuFu-Gli protein complexes.
552 *Journal Of Cell Biology* **191**: 415-428.
553 Villavicencio EH, Walterhouse DO, Iannaccone PM. 2000. The sonic hedgehog-
554 patched-gli pathway in human development and disease. *Am J Hum Genet* **67**:
555 1047-1054.
556 Woodruff JB, Ferreira Gomes B, Widlund PO, Mahamid J, Honigmann A, Hyman AA.
557 2017. The Centrosome Is a Selective Condensate that Nucleates Microtubules
558 by Concentrating Tubulin. *Cell* **169**: 1066-1077 e1010.
559 Yang XJ, Gregoire S. 2006. A recurrent phospho-sumoyl switch in transcriptional
560 repression and beyond. *Mol Cell* **23**: 779-786.
561 Zhou M, Han Y, Jiang J. 2023. Ulk4 promotes Shh signaling by regulating Stk36 ciliary
562 localization and Gli2 phosphorylation. *eLife* **12**.
563 Zhou M, Han Y, Wang B, Cho YS, Jiang J. 2022. Dose-dependent phosphorylation and
564 activation of Hh pathway transcription factors. *Life Sci Alliance* **5**.
565 Zhou M, Jiang J. 2022. Gli Phosphorylation Code in Hedgehog Signal Transduction.
566 *Front Cell Dev Biol* **10**: 846927.
567

568
569
570 **Figure 1. Stk36-mediated phosphorylation of Ulk4 suffices to drive its ciliary tip**
571 **accumulation**
572
573 (A-B) Representative images of immunostaining (A) and quantification (B) of ciliary tip
574 localized Ulk4-HA (green in A) in NIH3T3 cells infected with Ulk4 shRNA and lentivirus
575 expressing human Ulk4-WT-HA or Ulk4-EE-HA in the presence or absence of Shh-N.
576 (C-D) Representative images of immunostaining (C) and quantification (D) of ciliary tip
577 localized Ulk4-HA (green in C) or Myc-Stk36 (blue in C) in NIH3T3 cells infected with
578 Ulk4-WT-HA or Ulk4-EE-HA lentivirus. Primary cilia were marked by acetylated tubulin
579 (Ac-tub) staining (red in A and C). The intensity of ciliary-localized Ulk4-HA or Myc-
580 Stk36 was measured by Image J. 20 cells were randomly selected from each
581 experimental group for quantification. Data are mean ± SD from three independent
582 experiments. ***$p < 0.001$ (Student's t test). Scale bars are 5 μm.
583
584
585 **Figure 2. Stk36/Ulk4 promotes ciliary tip accumulation of Gli2 and Sufu**
586
587 (A-B) Representative images of immunostaining (A) and quantification (B) of ciliary tip
588 localized endogenous Sufu (green in A) or Gli2 (blue in A) in control or *Ulk3*^{KO} *Stk36*^{KO}
589 (DKO) NIH3T3 cells infected with Stk36-WT or Stk36-AA lentivirus and treated with or
590 without Shh-N.
591 (C-F) Representative images of immunostaining (C, E) and quantification (D, F) of
592 ciliary tip localized Ulk4-HA (green in C, E), Gli2 (blue in C) or Sufu (blue in E) in DKO
593 cells infected with Ulk4-WT-HA or Ulk4-EE-HA lentivirus.
594 Primary cilia were marked by acetylated tubulin (Ac-tub) staining (red in A, C and E).

595 The intensity of ciliary-localized Sufu, Gli2 or Ulk4-HA was measured by Image J. 20
596 cells were randomly selected from each experimental group for quantification. Data are
597 mean ± SD from three independent experiments. ***$p < 0.001$ (Student's t test). Scale
598 bars are 5 μm.

599
600
601 **Figure 3. Overexpression of phosphorylated Ulk4 drives its condensation outside**
602 **primary cilia**

603 (A-B) Representative images of immunostaining in HEK293T cells co-transfected with
604 the indicated Ulk4-HA and Fg-Stk36 expression constructs. Arrowheads indicate Ulk4
605 (green in A and B) and Stk36 (red in A and B) puncta.
606 (C) Representative images of immunostaining in HEK293T cells transfected with Ulk4-
607 EE-HA or Ulk4-AA-HA expression construct. Arrowheads indicate Ulk4-HA (green in C),
608 Gli2 (red in C) or Sufu (blue in C) puncta.
609 (D) Representative images of HEK293T cells expressing the indicated constructs before
610 and after treatment with 5% 1, 6-hexanediol for 5 minutes.
611 Scale bars are 6 μm.

612
613
614 **Figure 4. Stk36-mediated phosphorylation promotes Ulk4 SUMOylation**
615
616 (A-B) Western blot analysis of Ulk4 SUMOylation in HEK293T cells co-transfected with
617 the indicated Fg-Stk36 and Ulk4-HA constructs. Cells were lysed in the presence of the
618 deSUMOylation inhibitor NEM. Ulk4-HA was immunoprecipitated with anti-HA antibody,
619 followed by western blot analysis with HA and SUMO1 antibodies.

620 (C) Western blot analysis of Ulk4 SUMOylation in HEK293T cells transfected with Ulk4-
621 WT-HA or Ulk4-EE-HA construct and treated with or without TAK-981.
622 (D) Western blot analysis of Ulk4 SUMOylation in NIH3T3 cells infected with the
623 indicated Ulk4 constructs and treated with or without Shh-N.
624 (E) Schematic diagram of human Ulk4 with wild type and mutated sequences of Stk36
625 sites, SUMOylation site and SIM motif shown.
626 (F) *in vitro* phosphorylation and SUMOylation of Ulk4. GST-fusion proteins containing
627 wild type or mutant Ulk4C fragments were incubated with Fg-Stk36-EE purified from
628 HEK293T cells and recombinant CK1, followed by *in vitro* SUMOylation by incubating
629 with recombinant SUMO1, E1 and E2.
630 (G, H) Western blot analysis of Ulk4 SUMOylation in HEK293T cells co-transfected with
631 the indicated Fg-Stk36 and Ulk4-HA constructs.
632 (I) Western blot analysis of Ulk4 SUMOylation in NIH3T3 cells infected with Ulk4-WT-
633 HA or Ulk4-KR-HA construct and treated with or without Shh-N.
634 (J, K) Co-IP experiments to show Ulk4 self-association promoted by SUMO/SIM
635 interaction. HEK293T cells were transfected with the indicated Ulk4 constructs, followed
636 by immunoprecipitation and western blot analysis with the indicated antibodies.
637
638 **Figure 5. SUMOylation promotes Ulk4 condensation, ciliary tip accumulation, and**
639 **pathway activation depending on SIM**
640 (A) Representative images of immunostaining of HEK293T cells co-transfected with Fg-
641 Stk36-EE and Ulk4-WT-HA, Ulk4-KR-HA or Ulk4-ΔSIM-HA constructs. Arrowheads
642 indicate Ulk4 (green in A), Stk36 (red in A), or Gli2 (blue in A) puncta.

643 (B-C) Representative images of immunostaining (B) and quantification (C) of ciliary tip
644 localized Ulk4-HA (green in B) in NIH3T3 cells infected with Ulk4 shRNA and the
645 indicated human Ulk4 lentivirus in the presence or absence of Shh-N. Primary cilia were
646 marked by acetylated tubulin (Ac-tub) staining (red in A) and nuclei by DAPI (Blue in A).
647 (D) Western blot analysis of Myc-Gli2 phosphorylation on S230/S232 in NIH3T3 cells
648 expressing the control (Ctrl) or Ulk4 shRNA and the indicated Ulk4 lentiviral constructs
649 and treated with or without Shh-N.
650 (E-F) Relative *Gli1* (E) and *Ptch1* (F) mRNA levels in NIH3T3 cells expressing the
651 control (Ctrl) or Ulk4 shRNA and the indicated Ulk4 lentiviral constructs and treated with
652 or without Shh-N.
653 The intensity of ciliary localized wild type and mutant Ulk4-HA was measured by Image
654 J. 20 cells were randomly selected from each experimental group for quantification.
655 Data are mean ± SD from three independent experiments. ***$p < 0.001$ (Student's t
656 test).
657 Scale bars in A and B are 6 μm and 5 μm, respectively.
658
659
660 **Figure 6. Ulk4-EE exhibits constitutive Hh pathway activity depending on its**
661 **SUMOylation**
662 (A) Representative images of immunostaining of HEK293T cells transfected with the
663 indicated Ulk4 expression constructs and treated with or without the SUMOylation
664 inhibitor TAK981. Arrowheads indicate Ulk4 puncta. Scale bars are 6 μm.
665 (B, C) Representative images of immunostaining (B) and quantification (C) of ciliary tip
666 localized Ulk4-WT-HA or Ulk4-EE-HA (green) and endogenous Gli2 (blue) in NIH3T3

667 cells treated with or without the SUMOylation inhibitor TAK981. Primary cilia were
668 marked by acetylated tubulin (Ac-tub) staining (red). Scale bars are 5 μm.
669 (D) Representative images of immunostaining of HEK293T cells transfected with Ulk4-
670 EE-Fg or Ulk4-EE-KR-Fg expression construct. Arrowheads indicate Ulk4 puncta. Scale
671 bars are 6 μm.
672 (E, F) Representative images of immunostaining (E) and quantification (F) of ciliary tip
673 localized Ulk4-Fg (green) and endogenous Gli2 (blue) in NIH3T3 cells infected with
674 Ulk4-EE-Fg or Ulk4-EE-KR-Fg lentivirus. Primary cilia were marked by acetylated
675 tubulin (Ac-tub) staining (red). Scale bars are 5 μm.
676 (G, J) Western blot analysis of Myc-Gli2 phosphorylation on S230/S232 in NIH3T3 cells
677 co-infected with Myc-Gli2 and the indicated Ulk4 lentiviral constructs and treated with or
678 without the SUMOylation inhibitor TAK981.
679 (H, I, K, L) Relative *Ptch1* (H, K) and *Gli1* (I, L) mRNA levels in NIH3T3 cells infected
680 with the indicated Ulk4 lentiviral constructs and treated with or without the SUMOylation
681 inhibitor TAK981.
682 The intensity of ciliary-localized wild type and mutant Ulk4-HA was measured by Image
683 J. 20 cells were randomly selected from each experimental group for quantification.
684 Data are mean ± SD from three independent experiments. ***$p < 0.001$ (Student's t
685 test).
686
687 **Figure 7. Phosphorylation-induced SUMOylation promotes kinase/substrate**
688 **condensation at ciliary tip**

689 A working model in which Shh induces Ulk4/Stk36/Gli2/Sufu condensation at primary
690 cilia. In response to Shh, Stk36 phosphorylates Ulk4 on T1021/T1023, which induces
691 SUMOylation of Ulk4 on K1030. Subsequently, SUMO/SIM interaction drives the
692 formation of Ulk4 condensates at ciliary tip that recruit Stk36, Gli2, and Sufu.
693
694 **Figure 3-figure supplement 1. Stk36/Ulk4 condensates are resistant to 1, 6-**
695 **hexanediol**
696 Representative images of HEK293T cells expressing the indicated constructs before
697 and after treatment with 5% 1, 6-hexanediol for 10, 20, and 30 minutes.
698 Scale bars are 5 μm.
699
700 **Figure 7-figure supplement 1. The constitutive pathway activity of Ulk4-EE**
701 **depends on Stk36**
702 (A, B) Relative *Ptch1* (A) and *Gli1* (B) mRNA levels in NIH3T3 cells infected with the
703 indicated Ulk4 lentiviral constructs and treated with control (Ctrl) or Stk36 siRNA.
704 (C) Western blot analysis of Stk36 phosphorylation on pT158/pS159 in NIH3T3 cells co-
705 infected with the indicated Ulk4 and Stk36 lentiviral constructs.
706
707
708
709

Zhou_Fig1

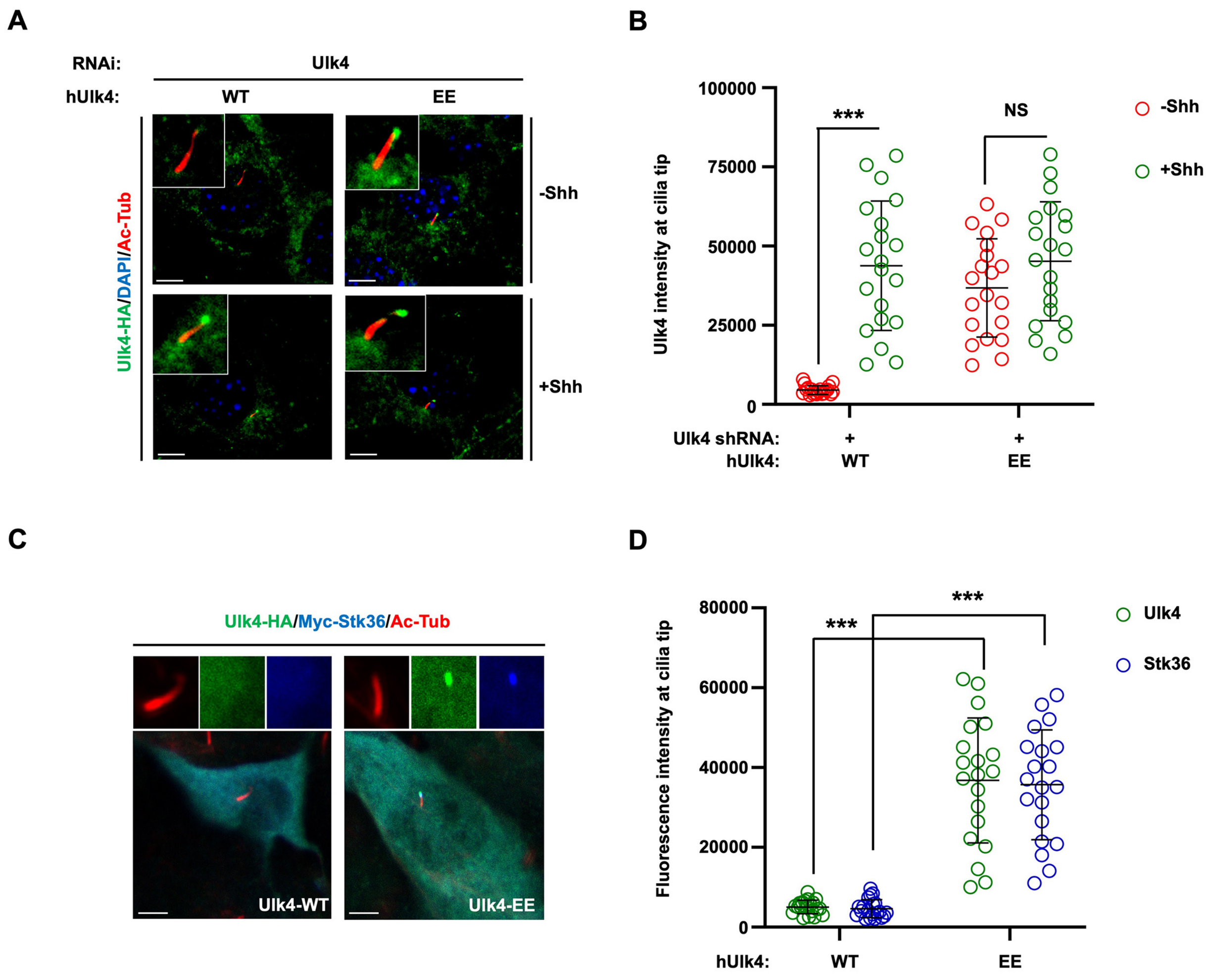
A
RNAi:
Ulk4
hUlk4:
WT
EE
Ulk4-HA/DAPI/Ac-Tub
-Shh
+Shh
B
Ulk4 intensity at cilia tip
100000
75000
50000
25000
0
***
NS
-Shh
+Shh
Ulk4 shRNA:
+
+
hUlk4:
WT
EE
C
Ulk4-HA/Myc-Stk36/Ac-Tub
Ulk4-WT
Ulk4-EE
D
Fluorescence intensity at cilia tip
80000
60000
40000
20000
0
***
***
Ulk4
Stk36
hUlk4:
WT
EE

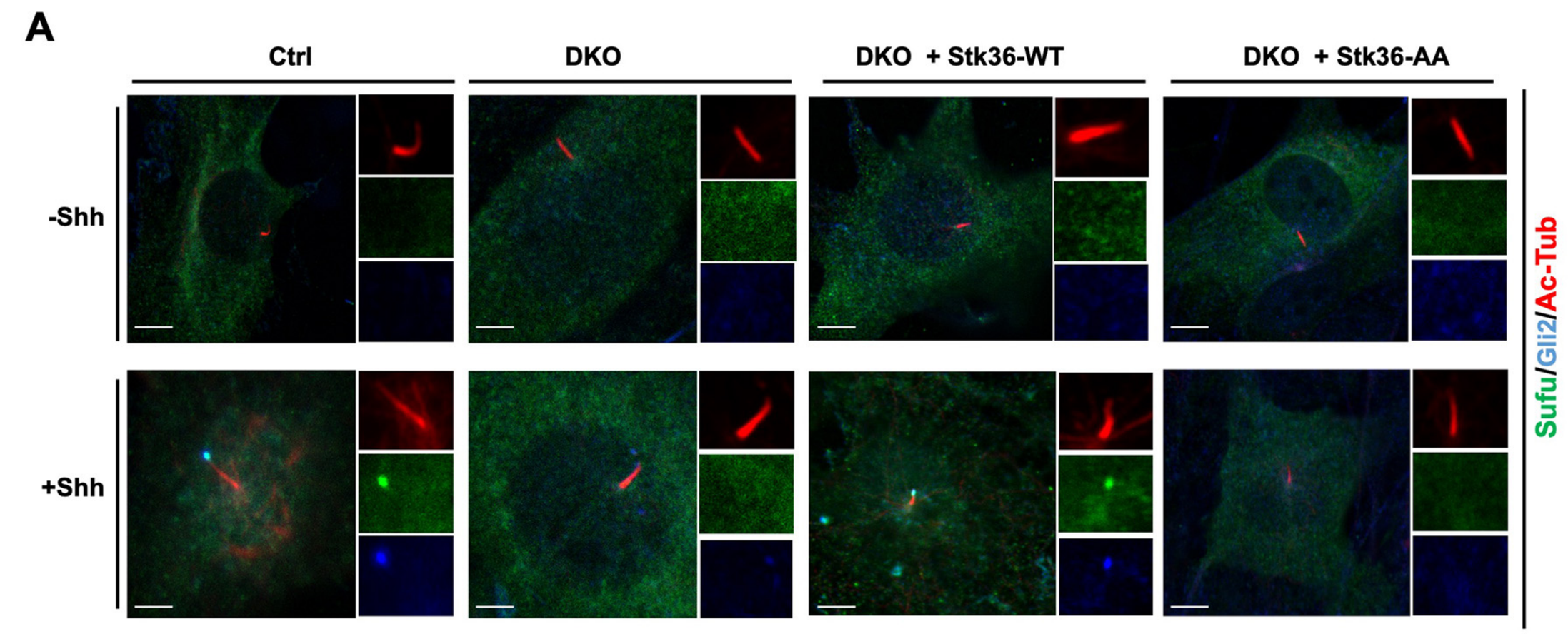
A
Ctrl
DKO
DKO + Stk36-WT
DKO + Stk36-AA
-Shh
+Shh
Sufu/Gli2/Ac-Tub

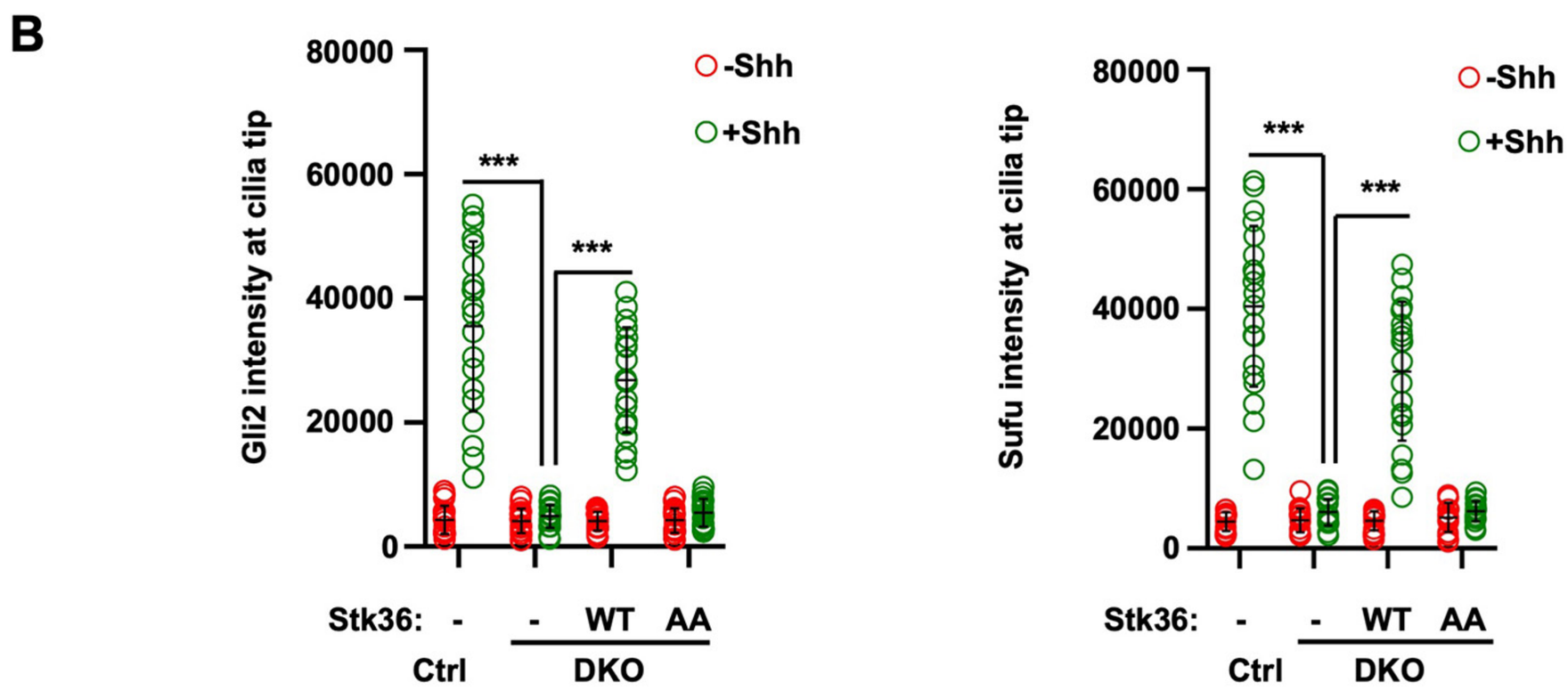
B
Gli2 intensity at cilia tip
80000
60000
40000
20000
0
-Shh
+Shh
***
***
Stk36: - - WT AA
Ctrl
DKO
Sufu intensity at cilia tip
80000
60000
40000
20000
0
-Shh
+Shh
***
***
Stk36: - - WT AA
Ctrl
DKO

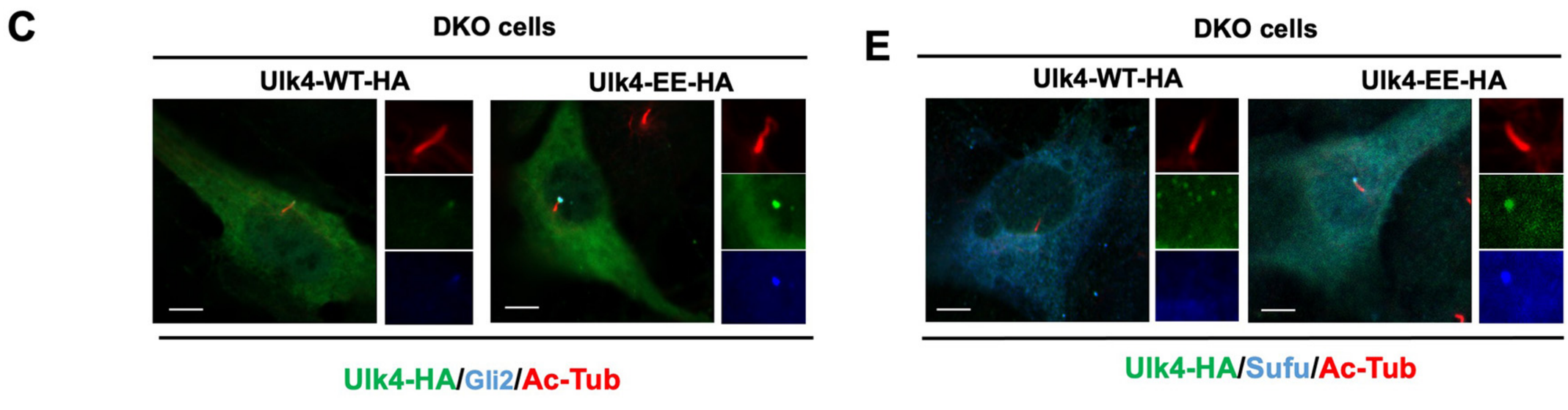
C
DKO cells
Ulk4-WT-HA
Ulk4-EE-HA
Ulk4-HA/Gli2/Ac-Tub
E
DKO cells
Ulk4-WT-HA
Ulk4-EE-HA
Ulk4-HA/Sufu/Ac-Tub

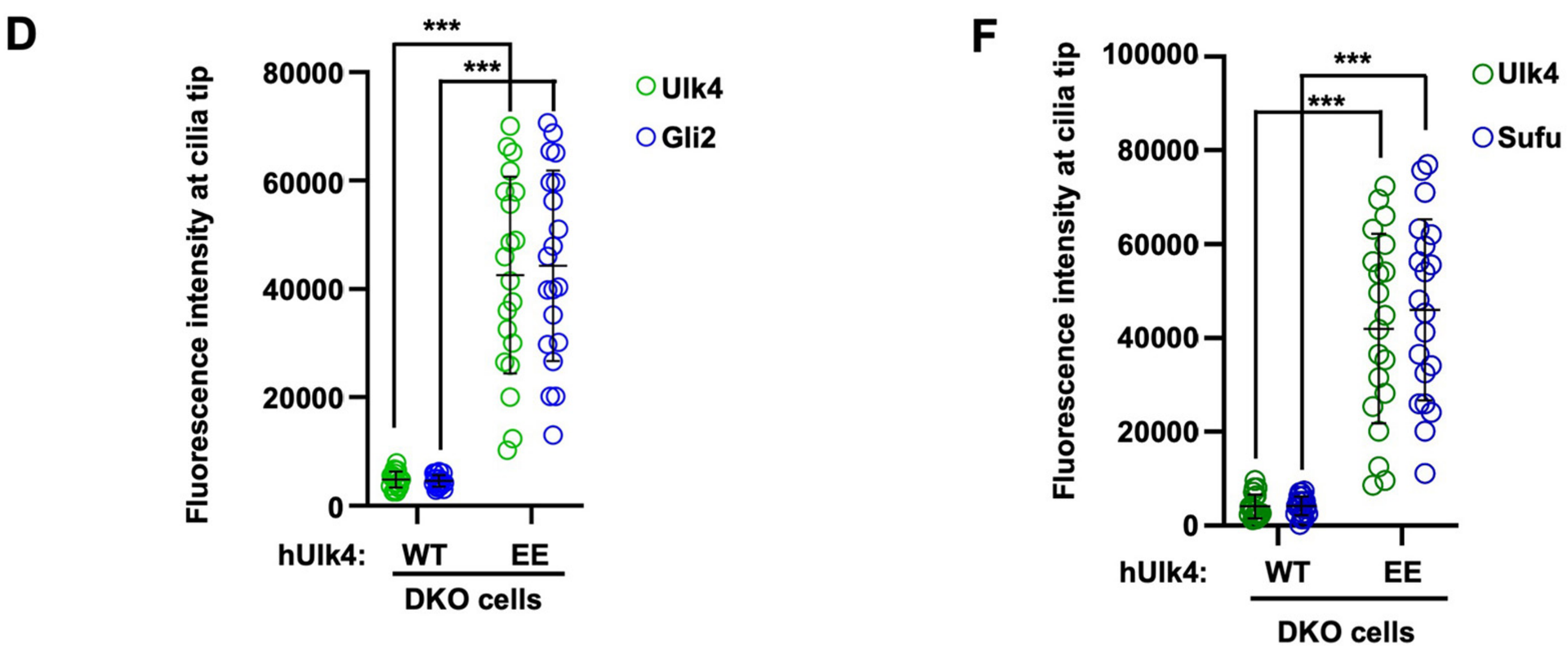
D
Fluorescence intensity at cilia tip
80000
60000
40000
20000
0
***
***
Ulk4
Gli2
hUlk4: WT EE
DKO cells
F
Fluorescence intensity at cilia tip
100000
80000
60000
40000
20000
0
***
***
Ulk4
Sufu
hUlk4: WT EE
DKO cells

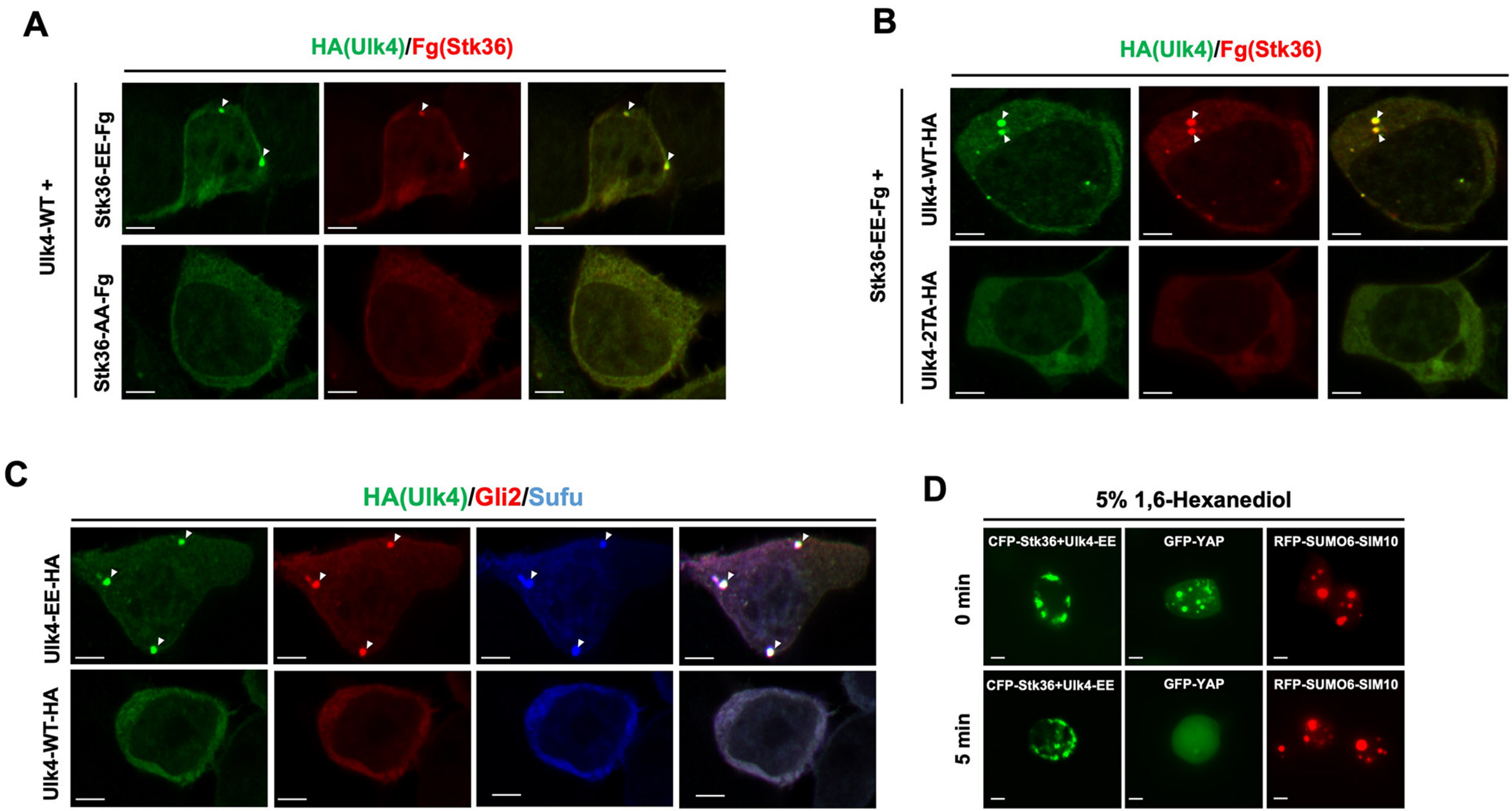
A
HA(Ulk4)/Fg(Stk36)
Ulk4-WT +
Stk36-EE-Fg
Stk36-AA-Fg
B
HA(Ulk4)/Fg(Stk36)
Stk36-EE-Fg +
Ulk4-WT-HA
Ulk4-2TA-HA
C
HA(Ulk4)/Gli2/Sufu
Ulk4-EE-HA
Ulk4-WT-HA
D
5% 1,6-Hexanediol
0 min
5 min
CFP-Stk36+Ulk4-EE
GFP-YAP
RFP-SUMO6-SIM10

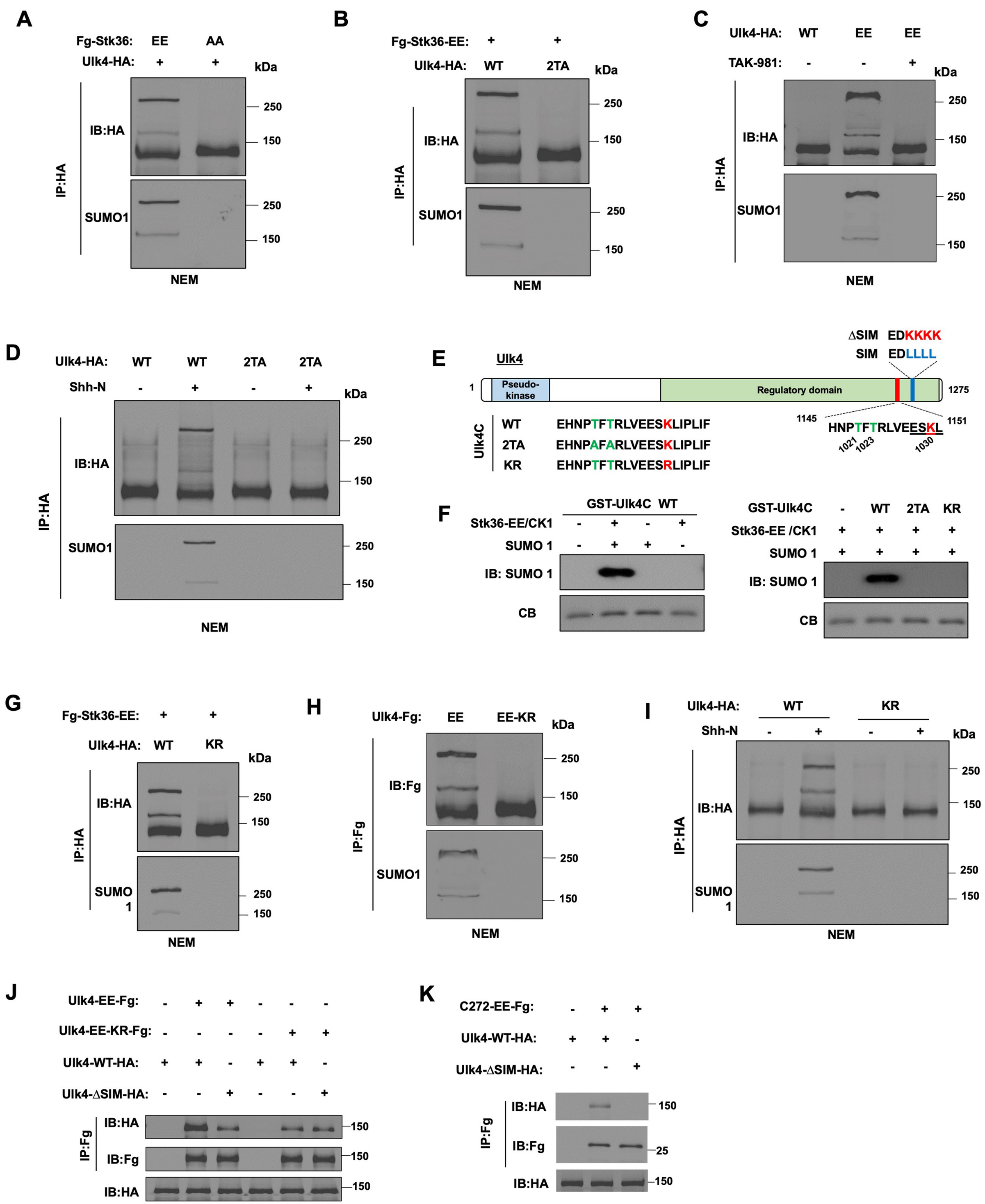
A
Fg-Stk36: EE AA
Ulk4-HA: + +
kDa
IB:HA
SUMO1
IP:HA
250
150
NEM
B
Fg-Stk36-EE: + +
Ulk4-HA: WT 2TA
kDa
IB:HA
SUMO1
IP:HA
250
150
NEM
C
Ulk4-HA: WT EE EE
TAK-981: - - +
kDa
IB:HA
SUMO1
IP:HA
250
150
NEM
D
Ulk4-HA: WT WT 2TA 2TA
Shh-N - + - +
kDa
IB:HA
SUMO1
IP:HA
250
150
NEM
E
Ulk4
1
Pseudo-kinase
Regulatory domain
1275
SIM EDLLLL
ΔSIM EDKKKK
Ulk4C
WT EHNPTFTRLVEESKLIPLIF
2TA EHNPAFARLVEESKLIPLIF
KR EHNPTFTRLVEESRLIPLIF
1145 HNPTFTRLVEESKL 1151
1021 1023 1030
F
GST-Ulk4C WT
Stk36-EE/CK1 - + - +
SUMO 1 - + + -
IB: SUMO 1
CB
GST-Ulk4C - WT 2TA KR
Stk36-EE /CK1 + + + +
SUMO 1 + + + +
IB: SUMO 1
CB
G
Fg-Stk36-EE: + +
Ulk4-HA: WT KR
kDa
IB:HA
SUMO 1
IP:HA
250
150
NEM
H
Ulk4-Fg: EE EE-KR
kDa
IB:Fg
SUMO1
IP:Fg
250
150
NEM
I
Ulk4-HA: WT KR
Shh-N - + - +
kDa
IB:HA
SUMO 1
IP:HA
250
150
NEM
J
Ulk4-EE-Fg: - + + - - -
Ulk4-EE-KR-Fg: - - - - + +
Ulk4-WT-HA: + + - + + -
Ulk4-ΔSIM-HA: - - + - - +
IB:HA
IB:Fg
IB:HA
IP:Fg
150
K
C272-EE-Fg: - + +
Ulk4-WT-HA: + + -
Ulk4-ΔSIM-HA: - - +
IB:HA
IB:Fg
IB:HA
IP:Fg
150
25
150

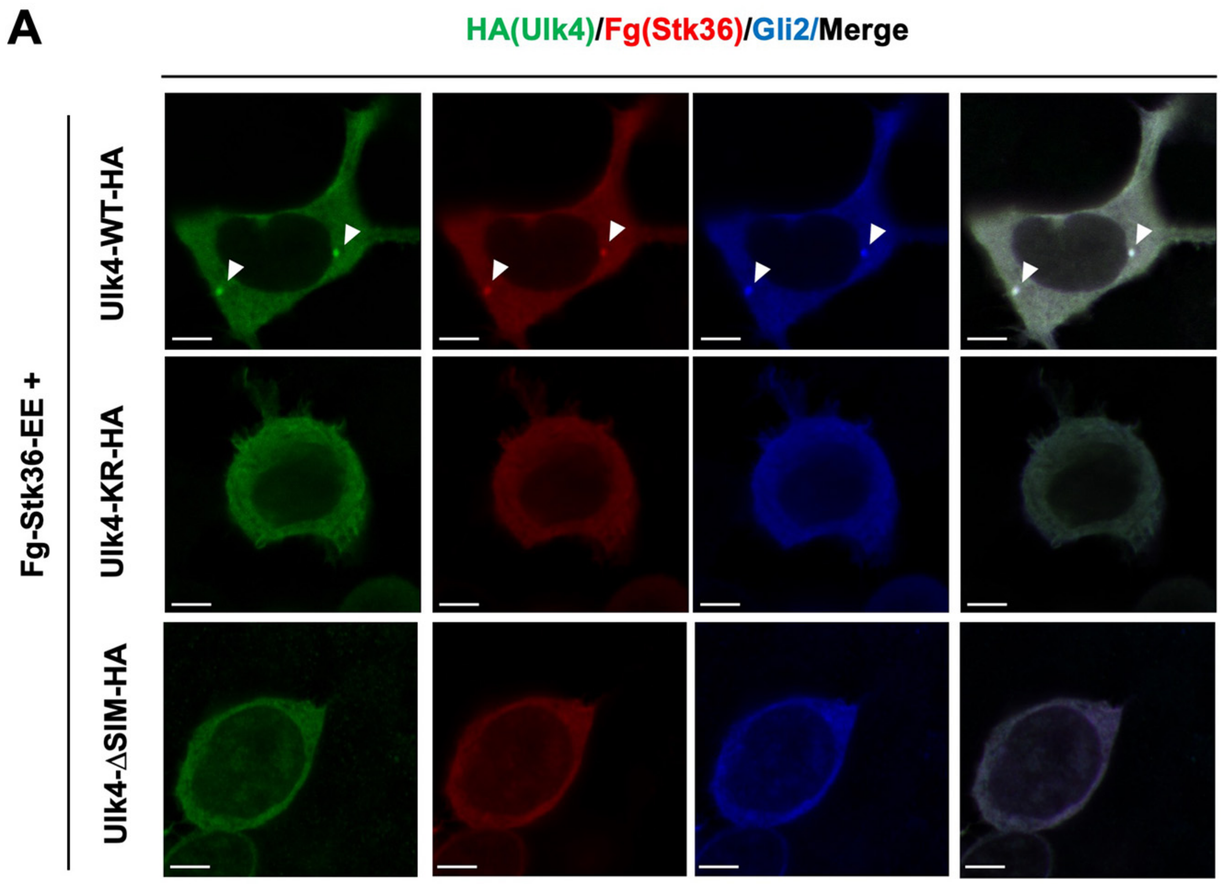
A
HA(Ulk4)/Fg(Stk36)/Gli2/Merge
Fg-Stk36-EE +
Ulk4-WT-HA
Ulk4-KR-HA
Ulk4-ΔSIM-HA

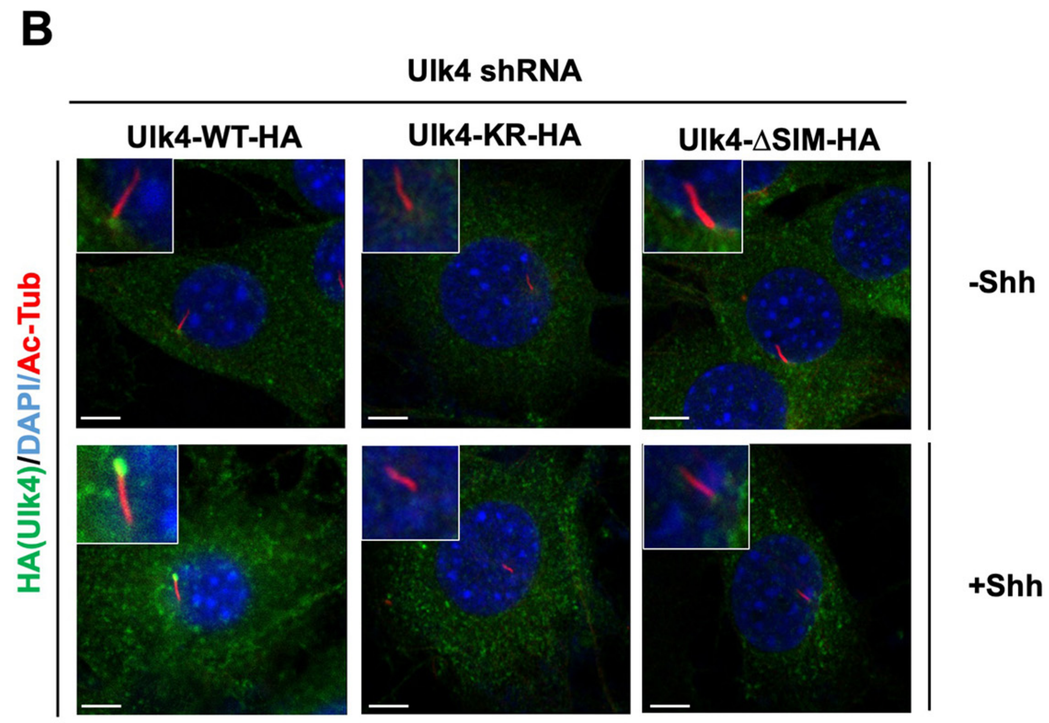
B
Ulk4 shRNA
Ulk4-WT-HA
Ulk4-KR-HA
Ulk4-ΔSIM-HA
HA(Ulk4)/DAPI/Ac-Tub
-Shh
+Shh

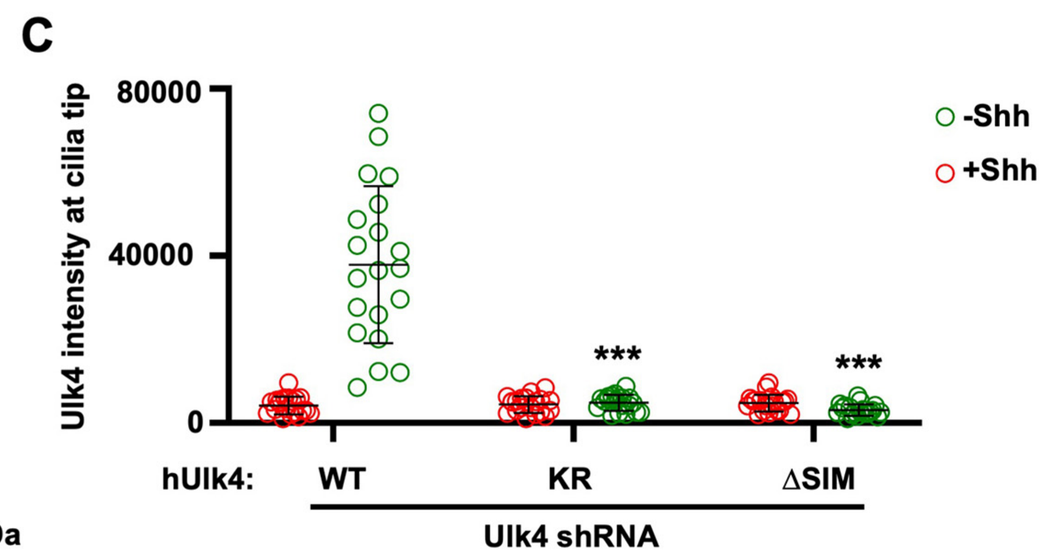
C
Ulk4 intensity at cilia tip
80000
40000
0
-Shh
+Shh
***
***
hUlk4:
WT
KR
ΔSIM
Ulk4 shRNA

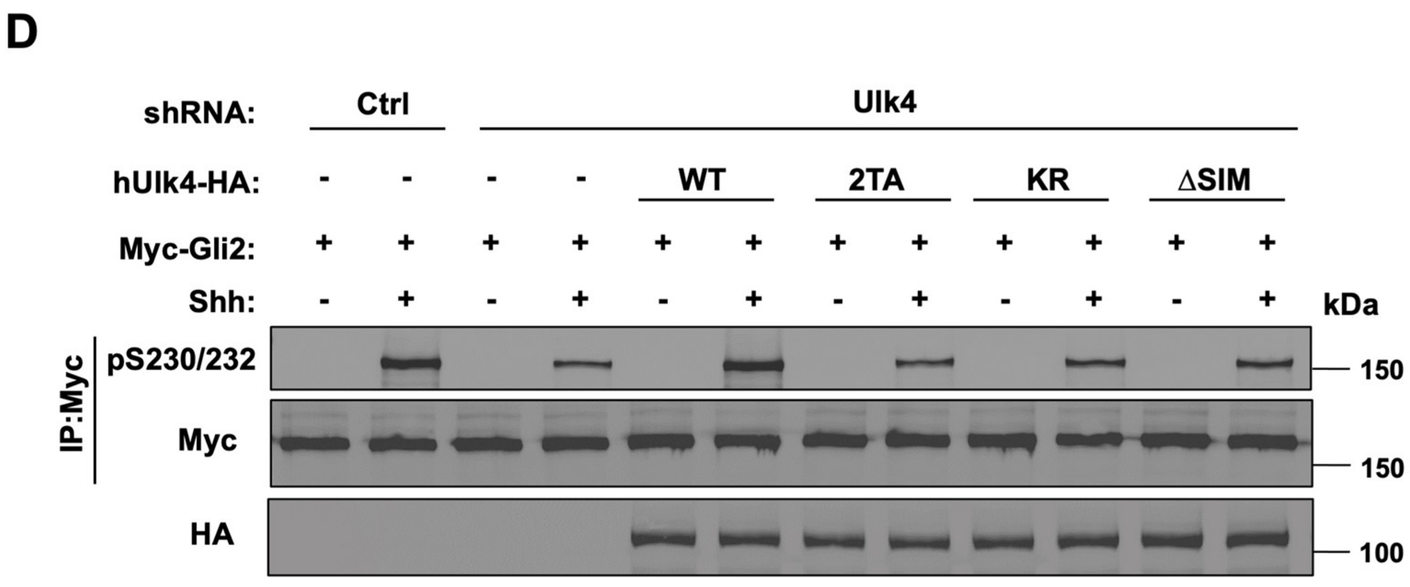
D
shRNA:
Ctrl
Ulk4
hUlk4-HA:
WT
2TA
KR
ΔSIM
Myc-Gli2:
Shh:
kDa
IP:Myc
pS230/232
Myc
HA
150
150
100

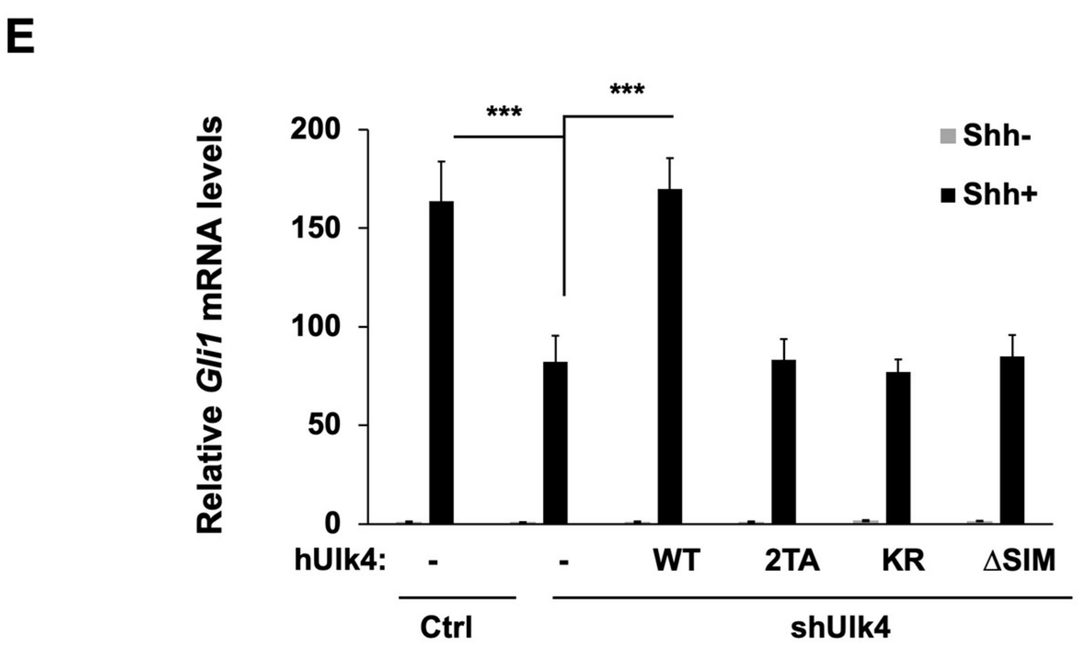
E
Relative Gli1 mRNA levels
200
150
100
50
0
***
***
Shh-
Shh+
hUlk4:
WT
2TA
KR
ΔSIM
Ctrl
shUlk4

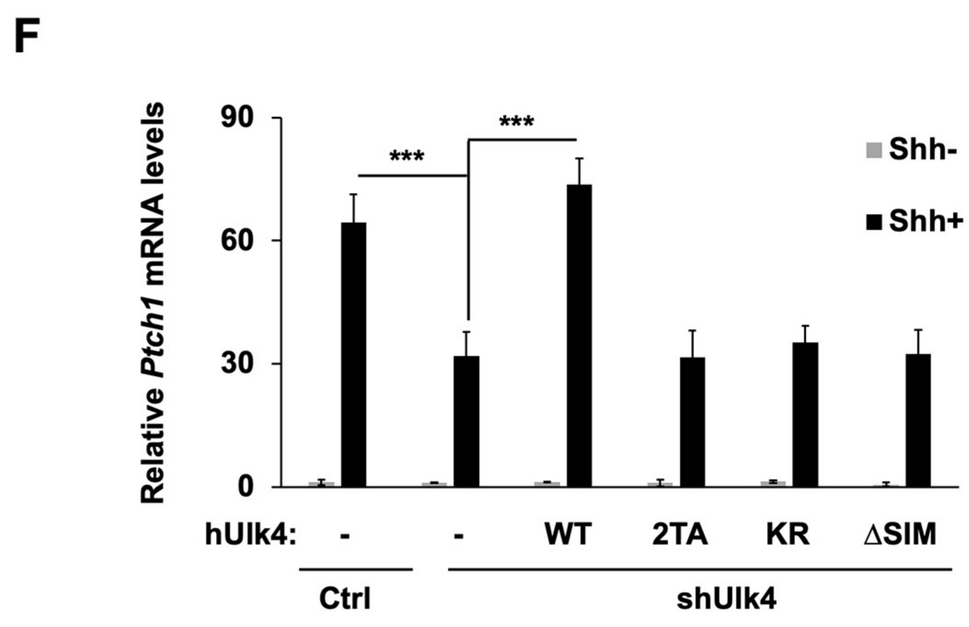
F
Relative Ptch1 mRNA levels
90
60
30
0
***
***
Shh-
Shh+
hUlk4:
WT
2TA
KR
ΔSIM
Ctrl
shUlk4

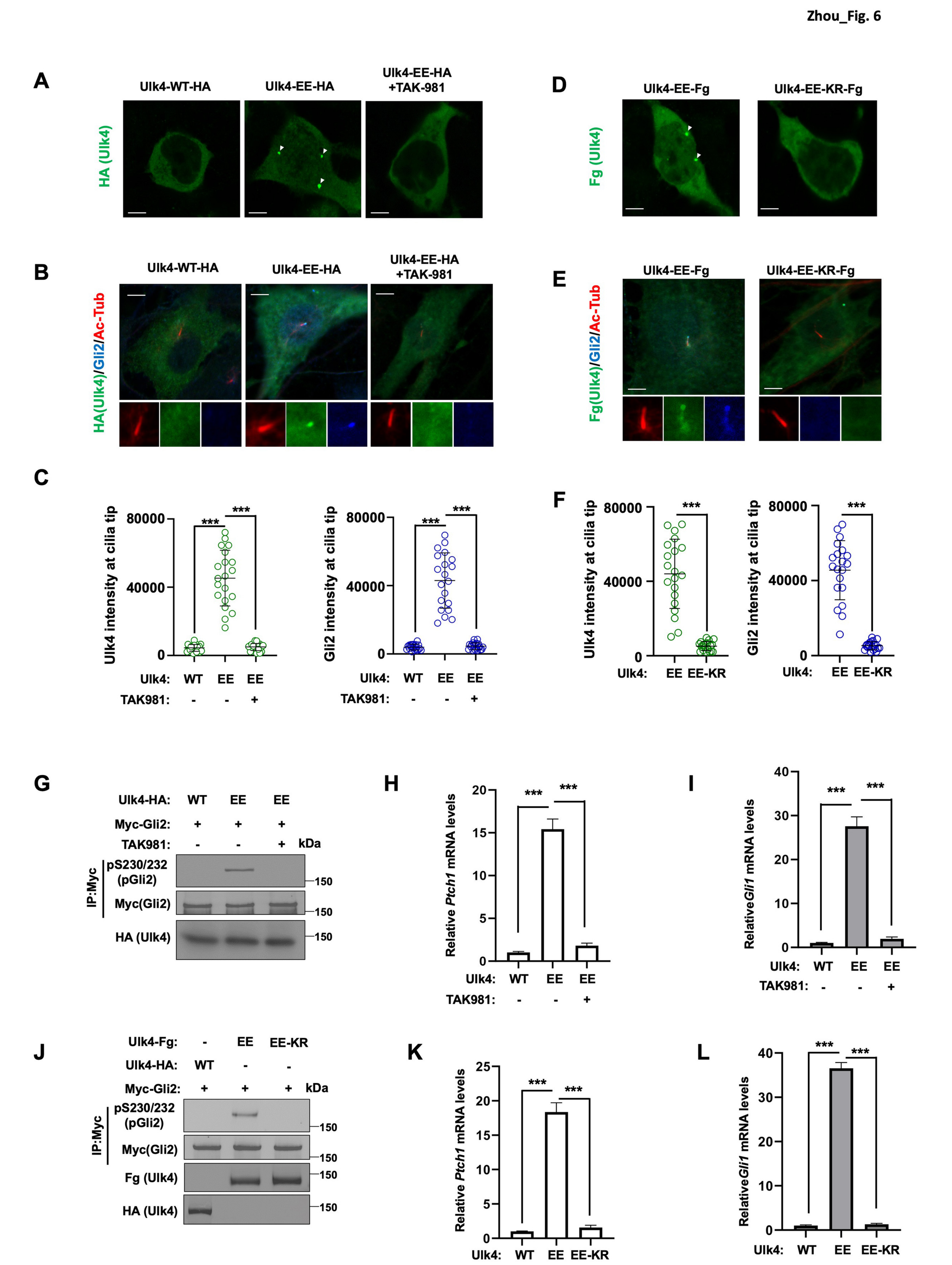
A
Ulk4-WT-HA
Ulk4-EE-HA
Ulk4-EE-HA +TAK-981
HA (Ulk4)
B
Ulk4-WT-HA
Ulk4-EE-HA
Ulk4-EE-HA +TAK-981
HA(Ulk4)/Gli2/Ac-Tub
C
Ulk4 intensity at cilia tip
Gli2 intensity at cilia tip
80000
40000
0
***
Ulk4: WT EE EE
TAK981: - - +
D
Ulk4-EE-Fg
Ulk4-EE-KR-Fg
Fg (Ulk4)
E
Ulk4-EE-Fg
Ulk4-EE-KR-Fg
Fg(Ulk4)/Gli2/Ac-Tub
F
Ulk4 intensity at cilia tip
Gli2 intensity at cilia tip
Ulk4: EE EE-KR
G
Ulk4-HA: WT EE EE
Myc-Gli2: + + +
TAK981: - - +
kDa
IP:Myc
pS230/232 (pGli2)
Myc(Gli2)
HA (Ulk4)
150
H
Relative Ptch1 mRNA levels
20
15
10
5
0
Ulk4: WT EE EE
TAK981: - - +
I
Relative Gli1 mRNA levels
40
30
20
10
0
Ulk4: WT EE EE
TAK981: - - +
J
Ulk4-Fg: - EE EE-KR
Ulk4-HA: WT - -
Myc-Gli2: + + +
kDa
IP:Myc
pS230/232 (pGli2)
Myc(Gli2)
Fg (Ulk4)
HA (Ulk4)
150
K
Relative Ptch1 mRNA levels
25
20
15
10
5
0
Ulk4: WT EE EE-KR
L
Relative Gli1 mRNA levels
40
30
20
10
0
Ulk4: WT EE EE-KR

Zhou_Fig.7

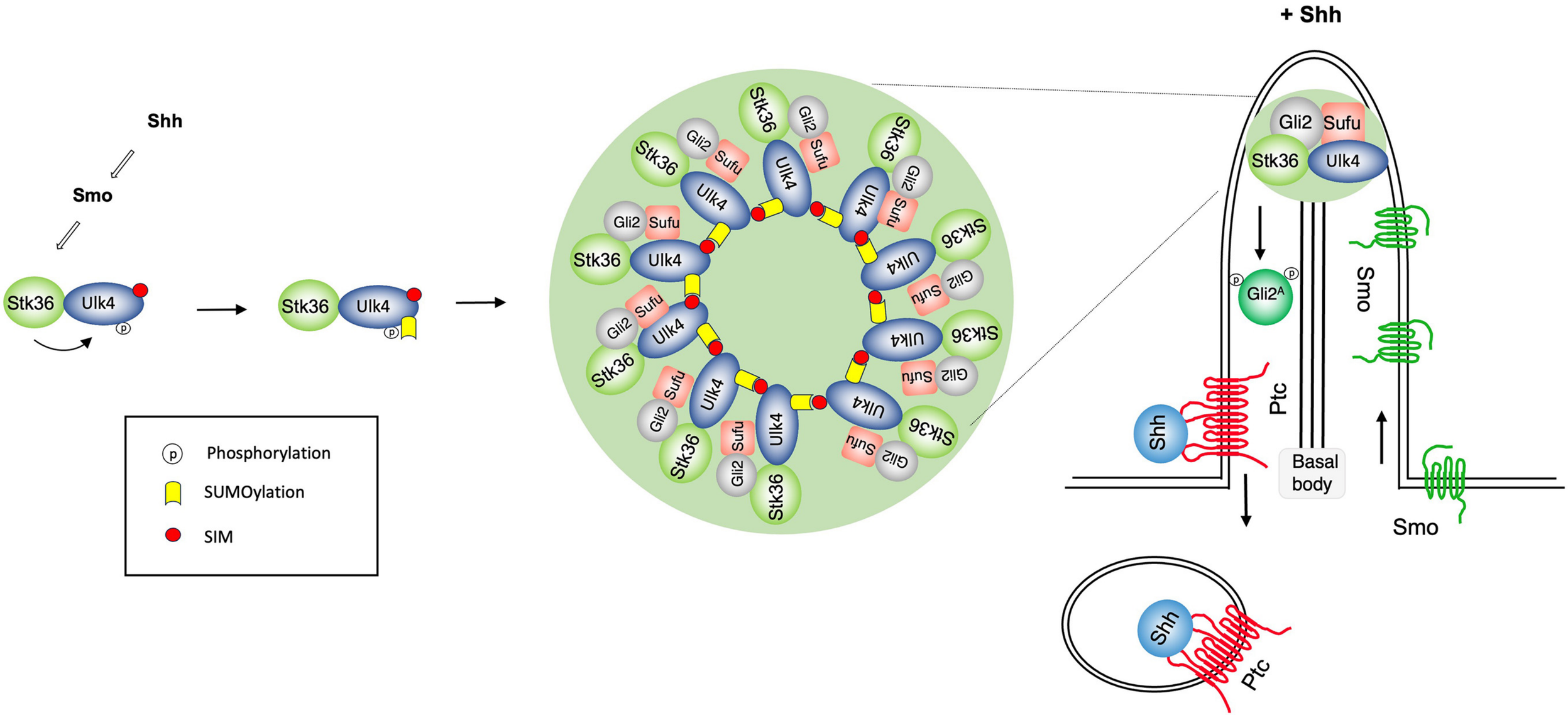
+ Shh
Shh
Smo
Stk36
Ulk4
p
Phosphorylation
SUMOylation
SIM
Gli2
Sufu
Gli2A
Ptc
Basal body
Smo

Figure3- figure supplement 1

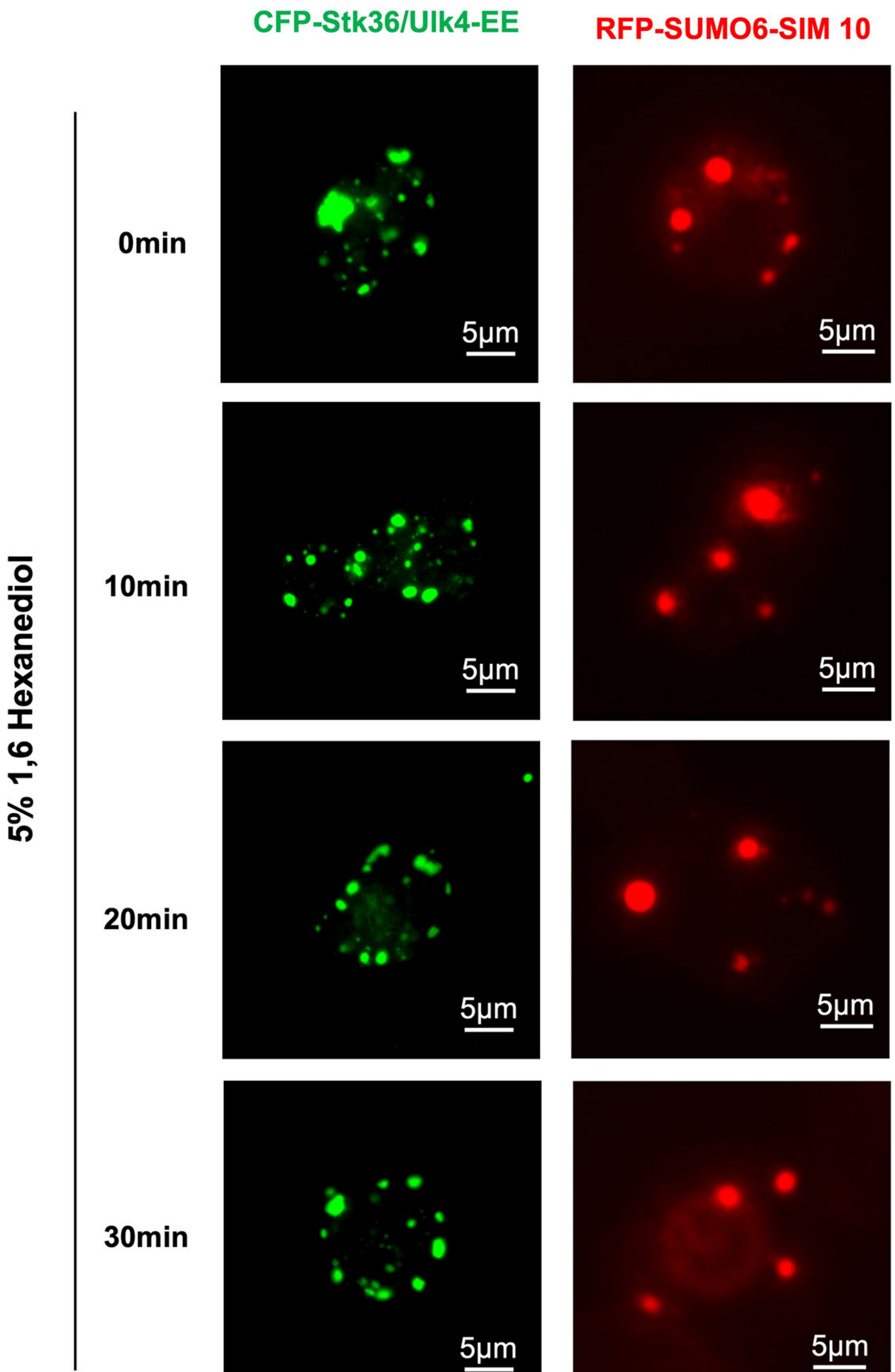
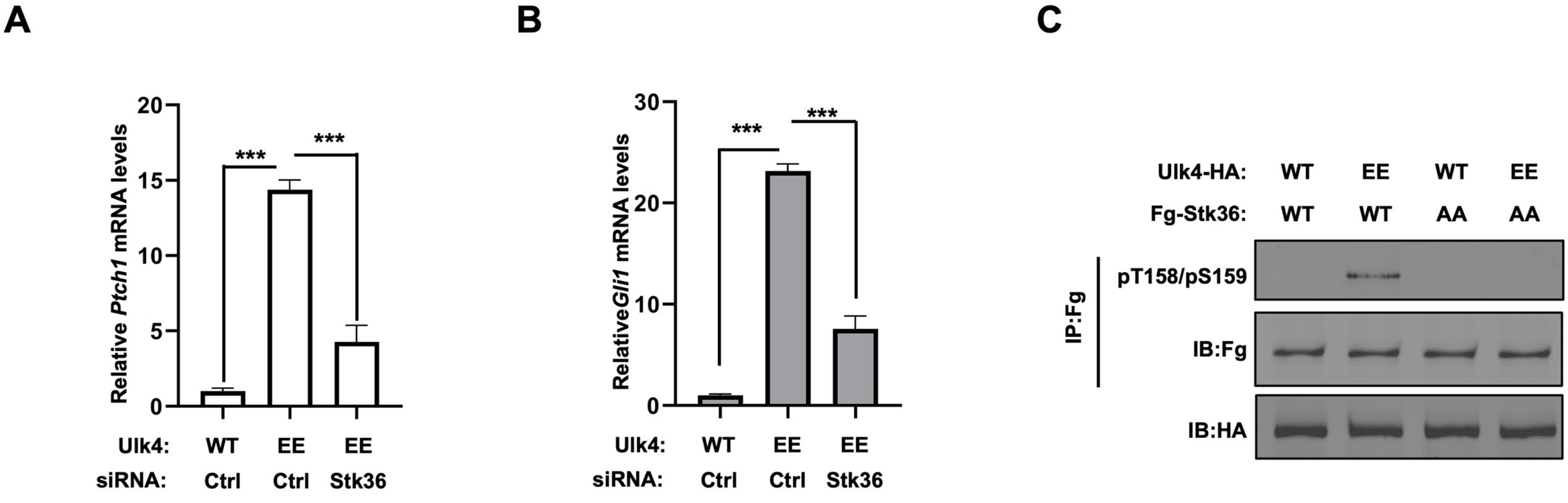
Figure 7-figure supplement 1